3. Crown heading with open invert

3.1 Glockenberg Tunnel near Koblenz, Germany

3.1.1 Introduction

In the course of the improvement of the federal highway 42 (B 42) between Bendorf and Lahnstein, Germany, the Glockenberg Tunnel was constructed on the side of the Rhine river opposite to the city of Koblenz.

This tunnel enables a non-intersecting access from the B 42 to the Pfaffendorf Rhine bridge. The southern portal of the tunnel lies in the direct extension of the Pfaffendorf Bridge. For each direction, the tunnel includes one driving lane, one stopping lane and an emergency sidewalk. In the mountain, the tunnel axis performs a 180° turn with a radius of ca. 50 m and then branches out into two single-lane tunnel tubes. One of these tubes accesses the B 42 in the direction of Bendorf, while the other one enables exiting the B 42 coming from Lahnstein into the direction of Koblenz (Fig. 3.1).

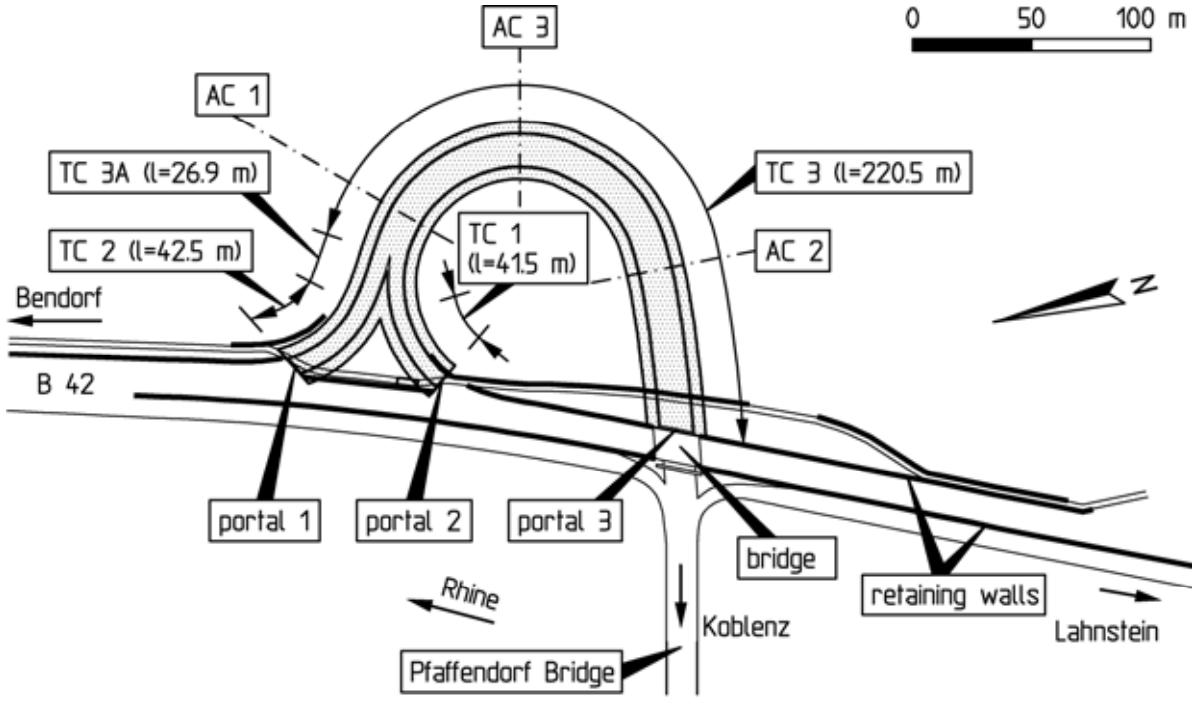

TC 1 - TC 3 and TC 3A: tunnel cross-sections

AC 1 - AC 3: analysis cross-sections

Fig. 3.1: Glockenberg Tunnel, site plan with analysis cross-sections

3.1.2 Structure

The 315 m long Glockenberg Tunnel was constructed by underground excavation starting at the southern portal 3 (Fig. 3.2). Up to location 220.5 m, the tunnel was excavated with the two-lane cross-section TC 3 shown in Fig. 3.3. From then on the cross-section was widened (TC 3A) up to chainage 248 m. In this way, the tunnel cross-section TC 3 is transformed into the two smaller tunnel tubes with the cross-sections TC 1 and TC 2. The smaller tunnel tubes each have a length of approx. 40 m and end at the portals 1 and 2 (Fig. 3.1).

Fig. 3.2: Glockenberg Tunnel, portal 3, crown

For the two-lane standard profile TC 3, a mouth-shaped profile with a width of 17.5 m and a height of 12 m was carried out. The excavated cross-section amounts to 175 m^2. The clearance is approx. 15 m wide and approx. 4.5 m high. The thickness of the shotcrete membrane is 25 cm, while the interior lining made from watertight concrete is 60 cm thick (Fig. 3.3).

In the vault area, a radius of curvature of R = 8.43 m was selected for the interior lining. The sidewalls were constructed with a radius of R = 4.66 m. With a radius of R = 25.25 m, the in-

vert was only slightly rounded out. For the transition from the sidewalls to the invert, a radius of R = 2.66 m was selected (Fig. 3.3).

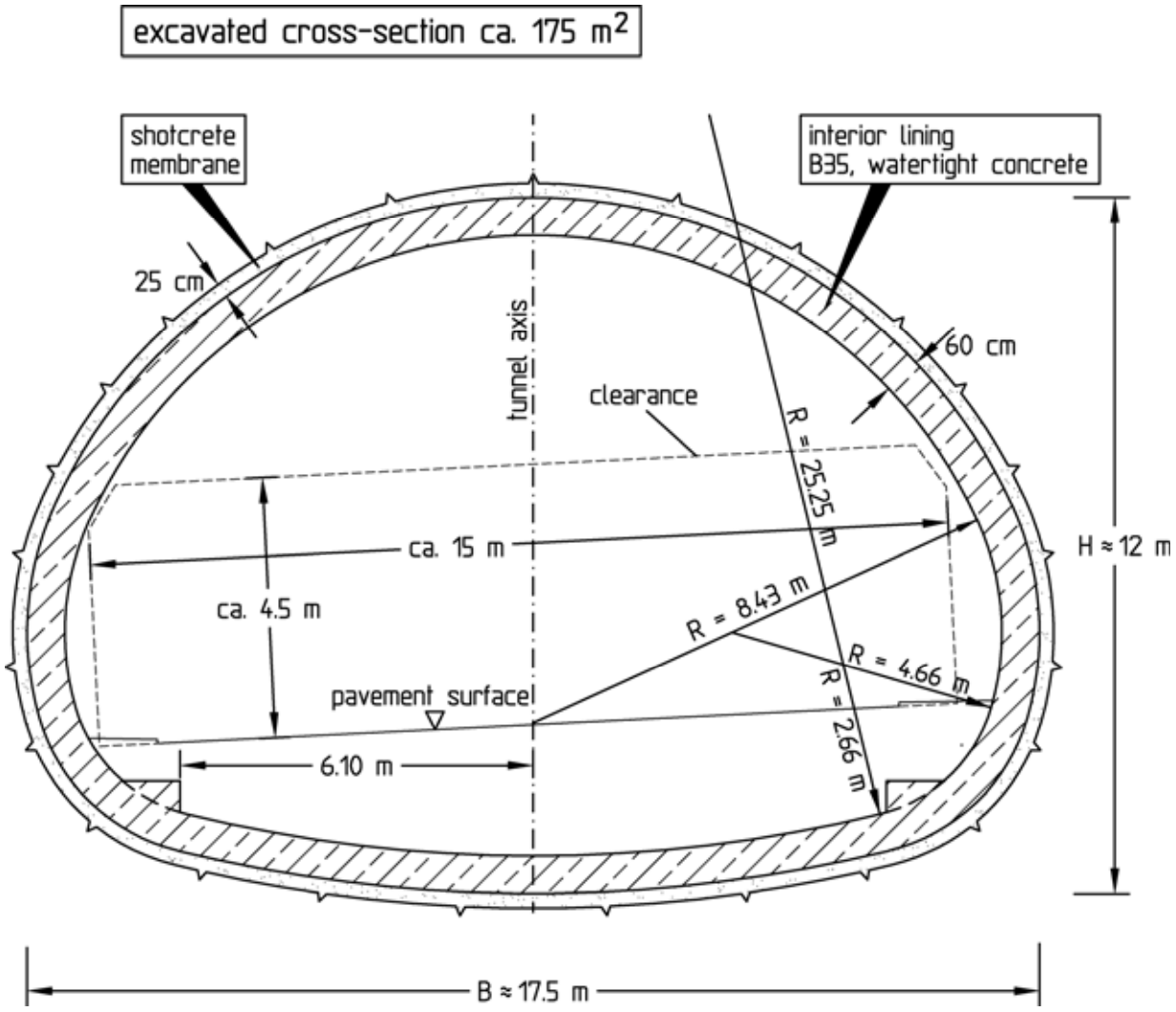

Fig. 3.3: Glockenberg Tunnel, tunnel cross-section TC 3

Fig. 3.4 shows the vertical section through the tunnel axis in the area of tunnel cross-sections TC3 and TC3A as a development. The maximum overburden height amounts to approx. 50 m.

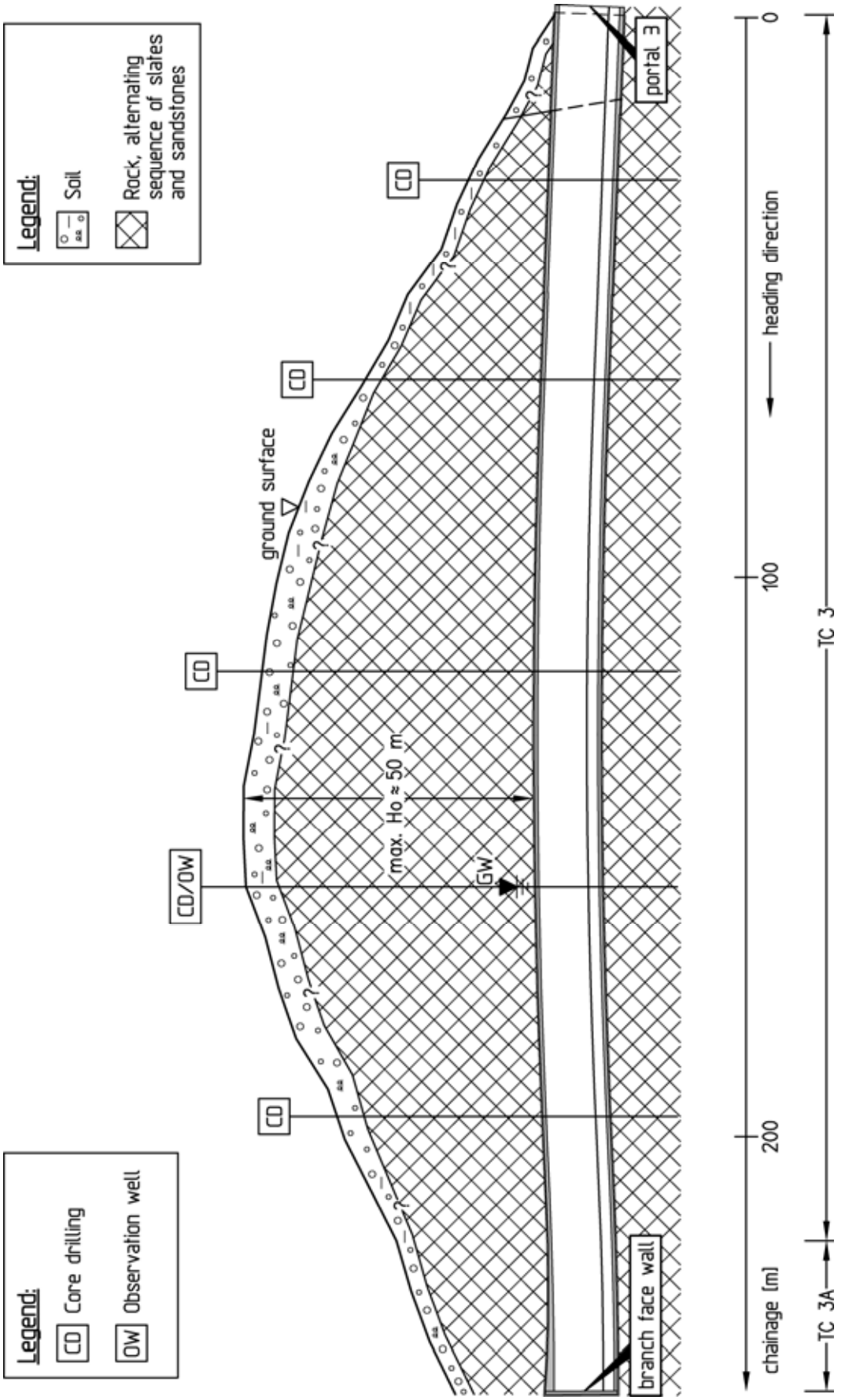

Fig. 3.4: Glockenberg Tunnel, vertical section through the tunnel axis, development

3.1.3 Ground and groundwater conditions

The ground along the alignment of the Glockenberg tunnel was explored using core drillings and test pits. One borehole was equipped as an observation well (Fig. 3.4).

According to the exploration, an up to 9 m thick soil layer consisting of talus material, residual detritus, loess and loess loam is underlain by an alternating sequence of slate and fine- to medium-grained sandstones belonging stratigraphically to the Lower Devonian of the Emsian stage (Fig. 3.4).

In the course of the Variscan orogenesis phase, the originally horizontal strata series were narrowed in NW-SE direction and bent to folds of different sizes. Within the large-scale folding structure, the alternating sequence of ribboned or flaser-like, locally secondarily silicated slates with sandstone banks up to several meters thick is in parts specially folded and sheared.

The sandstones are mostly quartzitically, locally also calcareously and ferrugineously cemented. Quartz and calcite veins millimeters to centimeters thick often occur in the rock zones rich in sand.

According to the results of the petrographic microscopy and X-ray diffractometry investigations, quartz, feldspar, mica and carbonates are the main rock-forming components.

The tunnel area is characterized by a distinct tectonic deformation in the form of a "special folding". Shallow as well as steep dipping of the strata to the northwest and southeast, respectively, occurs here with changes taking place over very short distances.

The rock is fractured by bedding-parallel discontinuities, the foliation and joints. As a result of the folding structure, the orientation of the discontinuities varies within the tunnel area. Fig. 3.5 shows the mean discontinuity orientations measured on oriented drill cores.

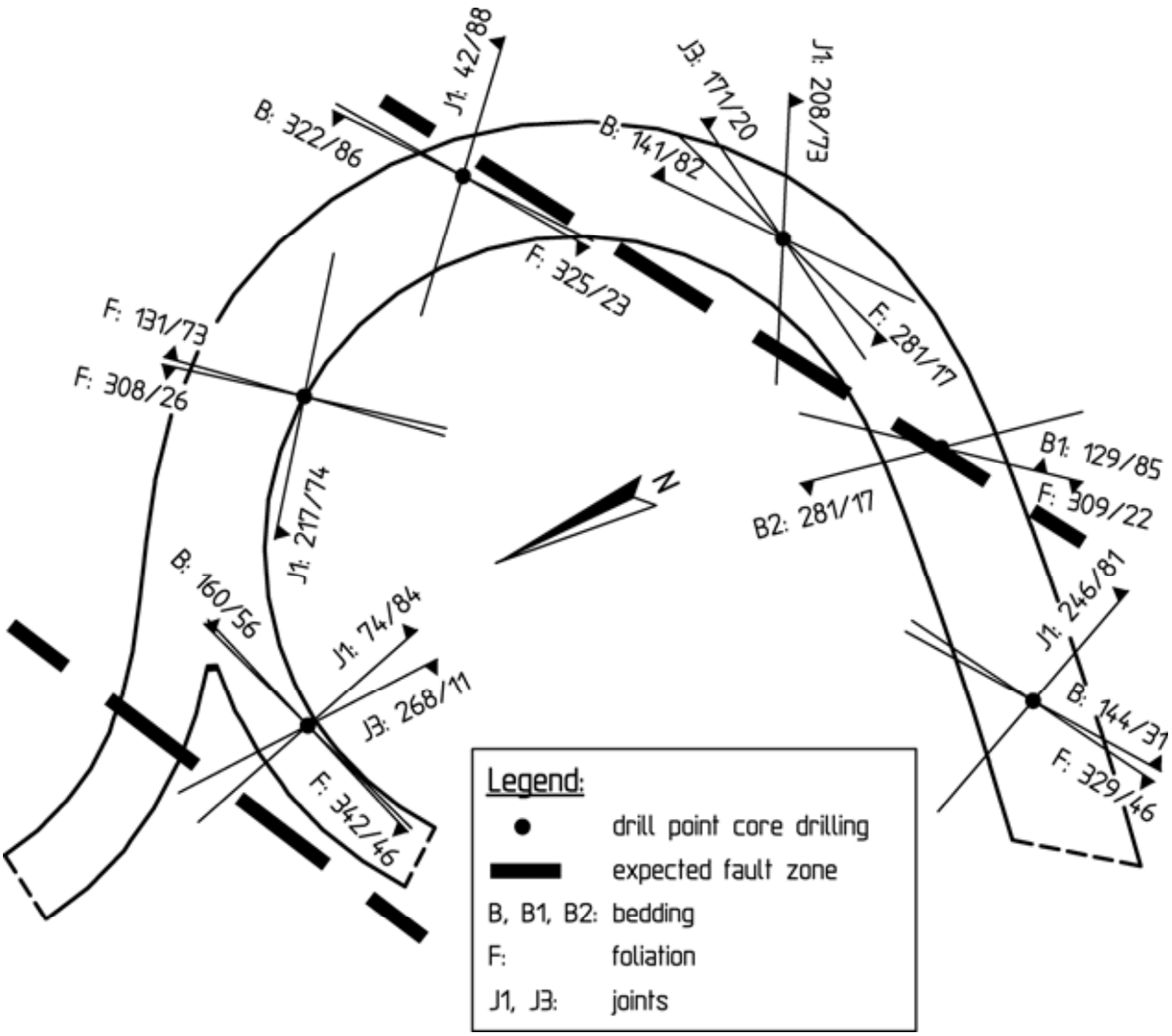

Fig. 3.5: Glockenberg Tunnel, site plan showing the orientation of the discontinuities and the location of the expected fault zones

As far as it can be assessed from the surface exposures, the bedding-parallel discontinuities must be assumed completely separated. Due to the exceeding of the shear strength on the bedding-parallel discontinuities as a result of shear during folding, triturated material and slickenside lineations locally exist on these planes. The same applies to quartz and calcite segregations which deposited in the cracks that developed due to dilatancy during the folding process.

Judging from surface exposures in the surroundings of the tunnel, the extension and the spacing of the foliation discontinuities depend distinctly on the appearance of the intact rock. In the case of greater thickness of the banks and mostly in the clayey rock

zones, individual completely separated foliation parallel discontinuities exist. Locally also slickenside lineations and triturated material were found on the foliation parallel discontinuities, indicating tectonic loading.

The joints contain many more rock bridges than the bedding- and foliation parallel discontinuities. Their degree of separation is correspondingly smaller.

In some core drillings, locally an increased core fragmentation, a more frequent appearance of slickensides parallel to the bedding or to the foliation, numerous quartz and calcite veins as well as rather strongly disintegrated rock zones were encountered. This led to the assumption that a fault zone striking in NE-SW direction in the area of tunnel cross-section TC 3 may be present (Fig. 3.5). Another fault zone was assumed in the area of tunnel cross-section TC 2 on the basis of the exploration results (Fig. 3.5).

Beneath the soil cover, which was encountered down to a depth of 9 m below ground surface during the exploration as mentioned above, the rock has only slightly been altered by weathering processes. An exception are more strongly fragmented rock zones, e. g. fault zones, in which weathering has clearly progressed.

To investigate the hydrological conditions, the groundwater level in the observation well OW (see Fig. 3.4) was measured and permeability tests were carried out at different depths in the boreholes.

The observation well was set up in the area in which the highest groundwater level was expected due to the location on the slope. The measurements showed that the groundwater is encountered here approx. 1 m above the tunnel roof (see Fig. 3.4).

3.1.4 Excavation classes

Because of the size of the excavated cross-section of approx. 175 m^2 (see Fig. 3.3), it was necessary to carry out excavation and support separately for crown, bench and invert (Fig. 3.6).

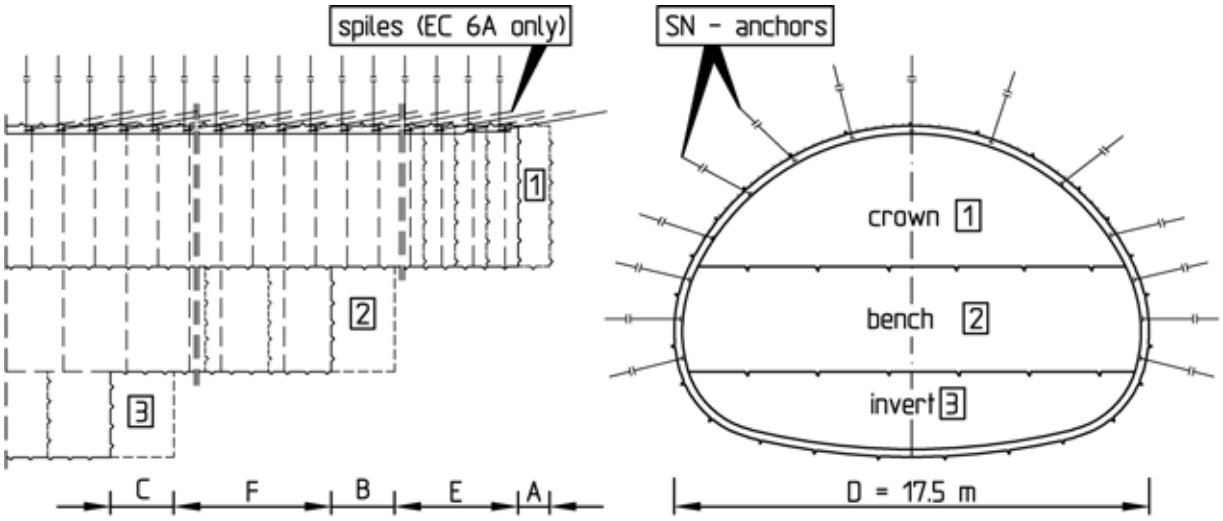

excavation class (EC)		4	5	6A
excavation method		smooth blasting / mechanical excavation	smooth blasting / mechanical excavation	smooth blasting / mechanical excavation
unsupported round length [m]	crown (A)	2	1.5	1.5
	bench (B)	4	3	3
	invert (C)	4	3	3
shotcrete B25		t = 25 cm	t = 25 cm	t = 25 cm
reinforcement		steel fabric mats Q295 (2 layers)	steel fabric mats Q295 (2 layers)	steel fabric mats Q295 (2 layers)
lattice girder spacing [m]	crown	2	1.5	1.5
	bench	4	3	3
systematic anchoring BSt 500S number, length	crown	7 pcs./round	7 pcs./round	9 pcs./round
		L = 4 m - 6 m, Φ = 25 mm		
	bench	12 pcs./round	10 pcs./round	12 pcs./round
		L = 4 m - 6 m, Φ = 25 mm		
tunnel face support		none	3 cm shotcrete, crown only	none
advance support		none	none	cemented spiles L_s = 4 m - 5 m $d_s \leq$ 35 cm
trailing distance	bench (E)	continuous crown heading, if bench and invert follow : E ≤ 2D and F ≤ 2D		
	invert (F)			

Fig. 3.6: Excavation classes 4, 5 and 6A for tunnel cross-section TC 3 (final design)

As already mentioned, a uniform orientation of the discontinuities could not be assumed. In addition, due to the circular tunnel

alignment, the orientation of the discontinuities relative to the tunnel axis changed continuously with the heading. Further, fault zones locally had to be expected (see Fig. 3.5). Therefore frequently varying rock conditions were assumed for the tender design and the final design. Correspondingly, the excavation classes 4, 5, 6A and 7A were specified in the final design in accordance with the recommendations of the working group "Tunneling" of the German Geotechnical Society (DGGT, 1995: Table 1).

A crown heading with an open invert was planned. The excavation class as well as the trailing distances of the bench excavation and the closing of the invert lining (E and F in Fig. 3.6) were to be selected in the course of the crown heading on the basis of the results of mapping and monitoring during construction (see Chapter 3.1.6). In this context special emphasis was placed on the results of the stability analyses (see Chapter 3.1.5) and of the geotechnical mapping.

The excavation methods, round lengths and support measures specified for the excavation classes 4, 5 and 6A for tunnel cross-section TC 3 in the final design are listed in Fig. 3.6. The excavation class 7A including advance support and support of the tunnel face was not carried out during construction.

Heading was planned by smooth blasting and/or mechanical excavation by a tunnel excavator and hydraulic chisel.

The unsupported round length during crown heading was selected as 2.0 m for excavation class 4 and 1.5 m for excavation classes 5 and 6A. In excavation class 6A an advance support of the crown with 4 to 5 m long mortar spiles was planned for every second round. Excavation class 5 included a sealing of the temporary crown face with shotcrete (Fig. 3.6).

For the shotcrete membrane, shotcrete of grade B25 with a thickness of 25 cm and two layers of reinforcing mats Q295 were specified. In the crown area, a systematic anchoring with 7 SN-anchors (excavation classes 4 and 5) resp. 9 SN-anchors (excavation class 6A) per round was planned. In each round a lattice girder was to be installed in the crown area (Fig. 3.6).

Due to reasons of construction management, a continuous crown heading was aimed for. If a trailing bench and invert should be-

come necessary for stability reasons, the maximum trailing distance E resp. F should amount to two tunnel diameters D (Fig. 3.6).

Unsupported round lengths for bench and invert of 4 m for excavation class 4 and 3 m for excavation classes 5 and 6A were planned. In the bench area, a systematic anchoring with 12 anchors (excavation classes 4 and 6A) resp. 10 anchors (excavation class 5) per round was specified. In each round one lattice girder was to be extended to the bench invert (Fig. 3.6).

The anchors were designed to be 4 to 6 m long in the crown as well as in the bench for all excavation classes (Fig. 3.6). If fault zones had to be crossed, locally longer anchors were planned to be installed.

3.1.5 Stability analyses

In order to investigate the stability and to dimension the shotcrete membrane, two-dimensional FE-analyses were carried out using the program system FEST03 (Wittke, 2000). Fig. 3.1 shows the analysis cross-sections AC 1, AC 2 and AC 3 investigated for the tunnel cross-section TC 3.

Because of the varying orientations of the discontinuities in the tunnel area and the changing direction of the tunnel axis due to the circular plan of the tunnel, four idealized structural models were established. All of them assume that the discontinuities strike parallel to the tunnel axis. They are thus on the conservative side with respect to the stability and the support measures ensuing from the analyses (see Fig. 3.5 and 3.7). Further, the dip angles of the discontinuities were varied over wide ranges (Fig. 3.7).

In model A, the bedding (B) and the foliation (F) are assumed dipping each at 45° perpendicular to the tunnel axis in opposite directions. In addition, a vertical joint set (J) striking parallel to the tunnel is taken into account. In model B the foliation is assumed dipping at 30° while the bedding dips at 60° in the opposite direction. Here as well an additional vertical joint set exists. Model C includes a vertical bedding striking parallel to the tunnel and a horizontal foliation. Instead of the vertical bedding planes, vertical joints are assumed in model D.

Aside from these different structural models, cases with a fault zone located in the area of the tunnel were investigated as well. Fig. 3.8 shows the assumed locations of these fault zones. Position L assumes a 5 m thick fault zone dipping at 70° close to the left side of the tunnel. With position M a vertical, 5 m thick fault zone running through the tunnel cross-section is taken into account. Position R assumes a 5 m thick fault zone dipping at 70° close to the right side of the tunnel.

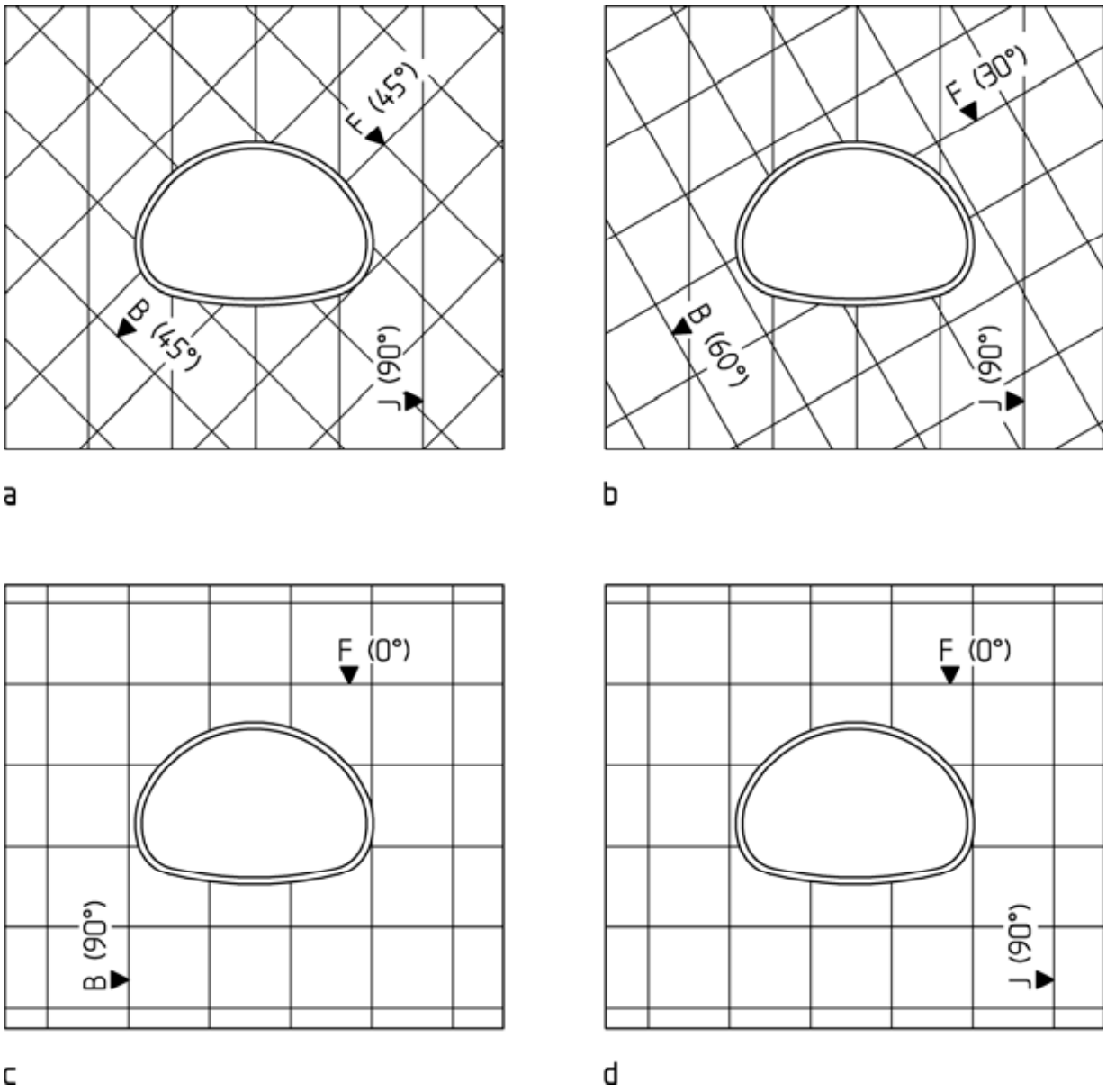

Fig. 3.7: Considered structural models: a) Model A; b) model B; c) model C; d) model D

In Fig. 3.9 and 3.10 the pseudo three-dimensional FE-mesh (slice with thickness of 1 m) used for analysis cross-section AC 3 is

shown. The FE-meshes for analysis cross-sections AC 1 and AC 2 have a corresponding setup, except for the overburden height.

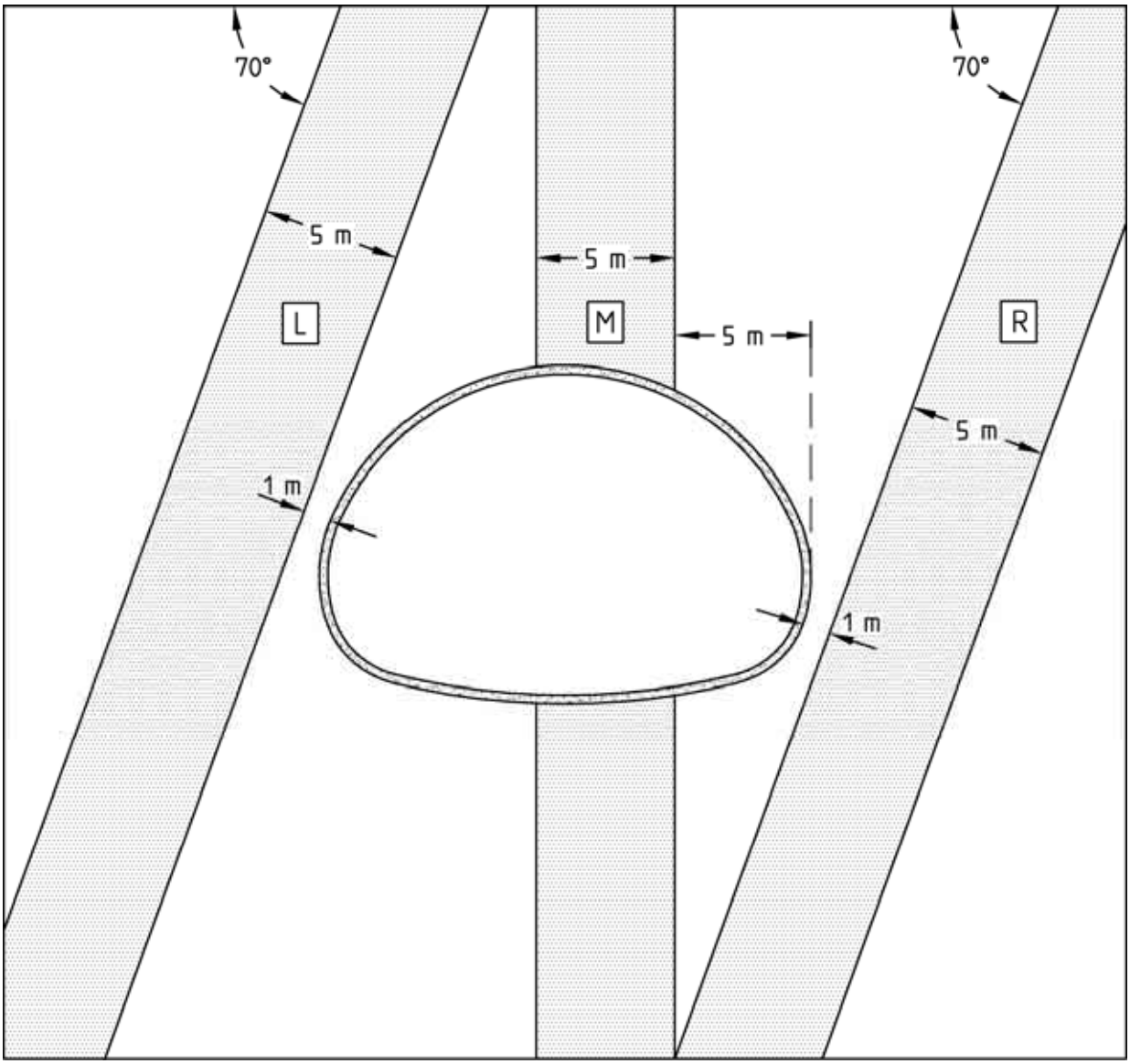

Fig. 3.8: Accounting for fault zones

The selected computation section is 140 m wide in transverse direction of the tunnel (x-direction). The height amounts to 120 m. The FE-mesh consists of 3288 three-dimensional, isoparametric elements with 7777 nodes (Fig. 3.9). The boundary conditions consist of vertically sliding supports for the nodes on the vertical boundary planes and of horizontally sliding supports for the nodes on the lower boundary plane (z = 0). All nodes are fixed in the y-direction.

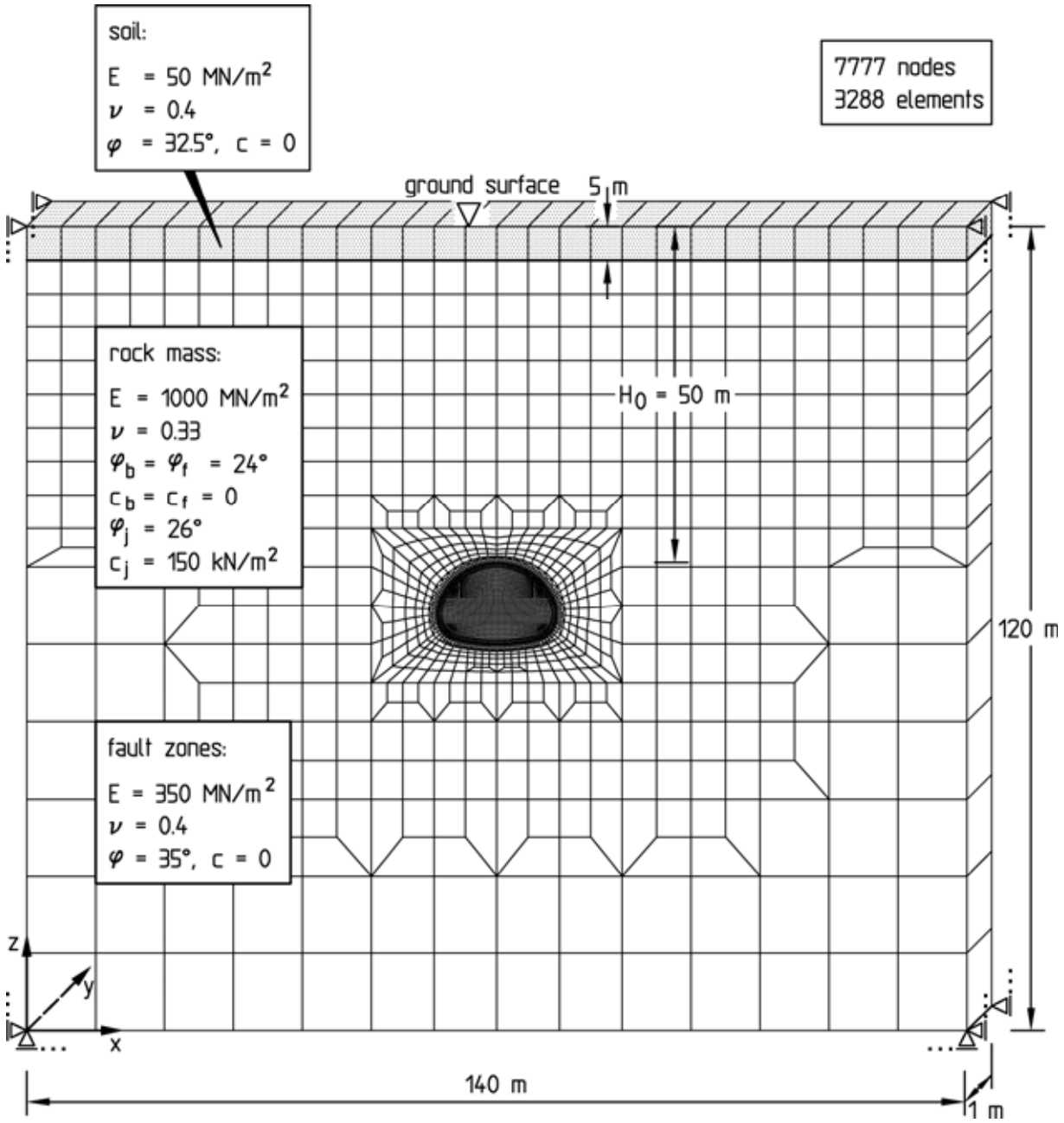

Fig. 3.9: Analysis cross-section AC 3, FE-mesh, boundary conditions, ground profile and parameters (reference case)

The setup of the ground layers is the same for all analysis cross-sections. The rock mass is encountered below a 5 m thick surface soil layer. In some analyses a fault zone in one of the positions shown in Fig. 3.8 is modeled discretely.

The parameters assumed in the stability analyses for the soil and the fault zone correspond to the specifications established during

the tender design. The rock mechanical parameters were specified in accordance with the parties concerned.

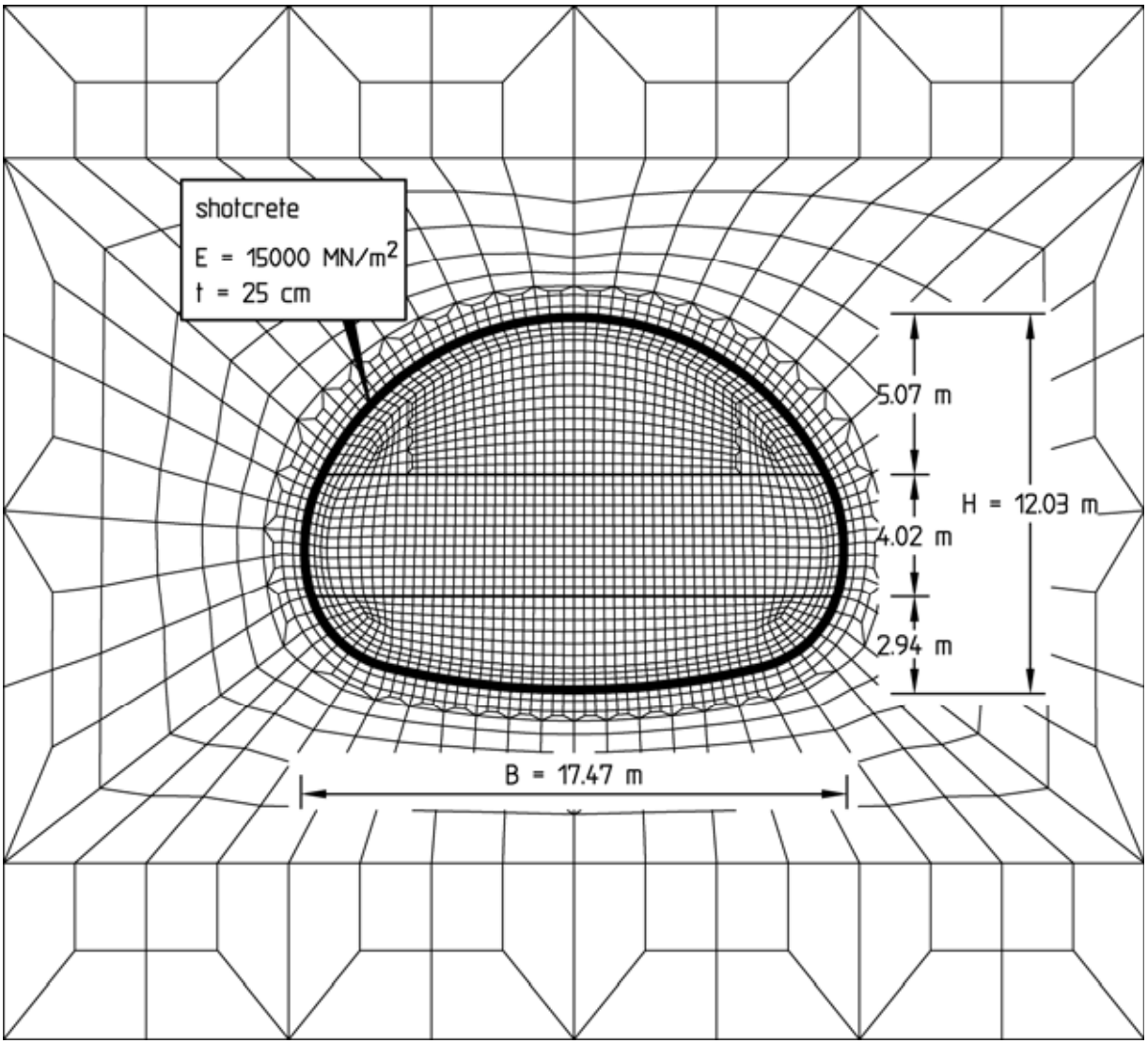

Fig. 3.10: Analysis cross-section AC 3, FE-mesh, detail

For the reference case, Young's modulus of the rock mass was assumed conservatively as E = 1000 MN/m^2. In comparative analyses a value of 1500 MN/m^2 was specified. Poisson's ratio was assumed as 0.33 (Fig. 3.9).

The angles of friction on the bedding-parallel and foliation parallel discontinuities were assumed as $\varphi_b = \varphi_f = 24°$. For the friction angle on the joints a value of $\varphi_j = 24°$ was selected (Fig. 3.9).

For the bedding parallel discontinuities no cohesion was assumed in all cases. The same applies to the foliation parallel discontinuities for the reference case (Fig. 3.9). In comparative analyses a cohesion of c_f = 100 kN/m^2 resp. c_f = 200 kN/m^2 was specified. The cohesion on the joints was selected as c_j = 150 kN/m^2 in the reference case (Fig. 3.9). In the comparative analyses it was assumed as c_j = 200 kN/m^2 and c_j = 300 kN/m^2, respectively.

The transfer of tensile stresses perpendicular to the discontinuities was excluded in all analysis cases.

A value of 15000 MN/m^2 was specified as statically effective Young's modulus of the shotcrete. This value is to include the hardening during the application of the load (see Chapter 2.1.5). As mentioned before, the thickness of the shotcrete membrane was selected as t = 25 cm (Fig. 3.10, see also Fig. 3.3 and 3.6).

The analyses were based on elastic-viscoplastic stress-strain behavior (Wittke, 2000) of the ground and elastic stress-strain behavior of the shotcrete membrane.

According to the findings of the exploration, locally a ground water table lying above the tunnel roof had to be expected. With the drainage during tunnel excavation, the ground water table is lowered to the level of the tunnel invert. There was no water pressure therefore to be considered in the stability analyses for the shotcrete membrane.

Fig. 3.11 shows a schematic representation of the computation steps for the simulation of the construction stages "crown excavation" and "bench excavation" and the excavation of the full cross-section.

The first computation step includes the computation of the state of stress and deformation resulting from the dead weight of the ground (in-situ state).

In the computation steps preceding the simulation of the individual partial excavations (computation steps 2, 4 and 6), a preceding stress relief is accounted for in the respective cross-section area to be excavated (Wittke, 2000).

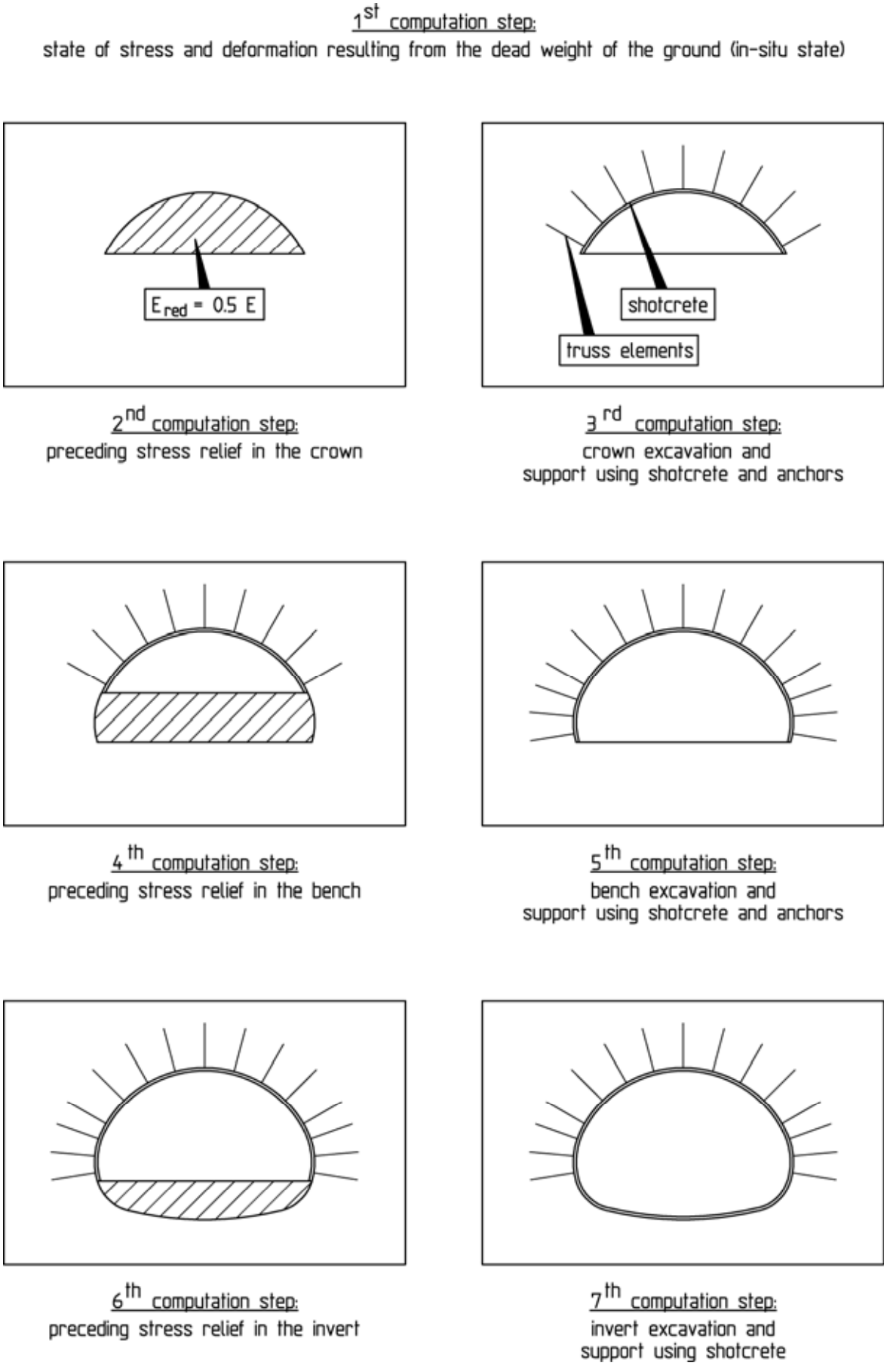

Fig. 3.11: Analysis cross-section AC 3, computation steps

To this end, Young's modulus in this area is reduced to the value $E_{red} = a_v \cdot E$ where E denotes Young's modulus of the ground and $a_v < 1.0$ is the so-called stress-relief factor. The preceding stress relief enables an approximate representation of the deformations and stress redistributions occurring in the rock preceding the tunnel excavation and the installation of the support. Due to the preceding stress relief, the shotcrete membrane installed in the following computation step is subjected to a smaller loading compared to a simultaneous simulation of excavation and installation of the shotcrete support without the intermediate step of the preceding stress relief. The stress relief factor is specified on the basis of experience gained from measurements on completed structures and comparisons with the results of three-dimensional analyses. In the present case, the preceding stress relief factor was chosen as $a_v = 0.5$ (Fig. 3.11).

In addition to the installation of the shotcrete membrane, the installation of the SN-anchors in crown and bench for excavation class 6A (see Fig. 3.6) is simulated in computation steps 2 (crown excavation and support) and 4 (bench excavation and support). The anchors are modeled by 4 m long truss elements (Wittke, 2000; Fig. 3.11).

In the following, the results of stability analyses for analysis cross-section AC 3 (see Fig. 3.1, 3.9 and 3.10) are shown exemplarily.

Analysis cross-section AC 3 is located in the area of the maximum overburden of approx. 50 m (Fig. 3.9). In this area the occurring discontinuity orientations can be captured approximately with structural models B and C (see Fig. 3.7).

The construction stage after the bench excavation (5^{th} computation step) proves to be critical with respect to the stability of the tunnel, if structural model B and the parameters given in Fig. 3.9 are assumed. If the anchors are not taken into account, the displacements do not converge in the course of the viscoplastic iterative calculation in the 5^{th} computation step, i. e. the stability of the tunnel cannot be proven by the analysis for this construction stage. Even if the anchors are taken into account, considerable viscoplastic displacements still result in this computation step, especially at the left bench lining toe. These displacements converge, however, in the course of the viscoplastic

iterative calculation. Fig. 3.12 and 3.13 show the principal normal stresses, the areas where the shear strength on the discontinuities is exceeded and the displacements of the excavation profile computed for the bench excavation with the anchors taken into account. The computed roof subsidence amounts to approx. 40 mm, the maximum heave of the invert to approx. 65 mm (Fig. 3.13).

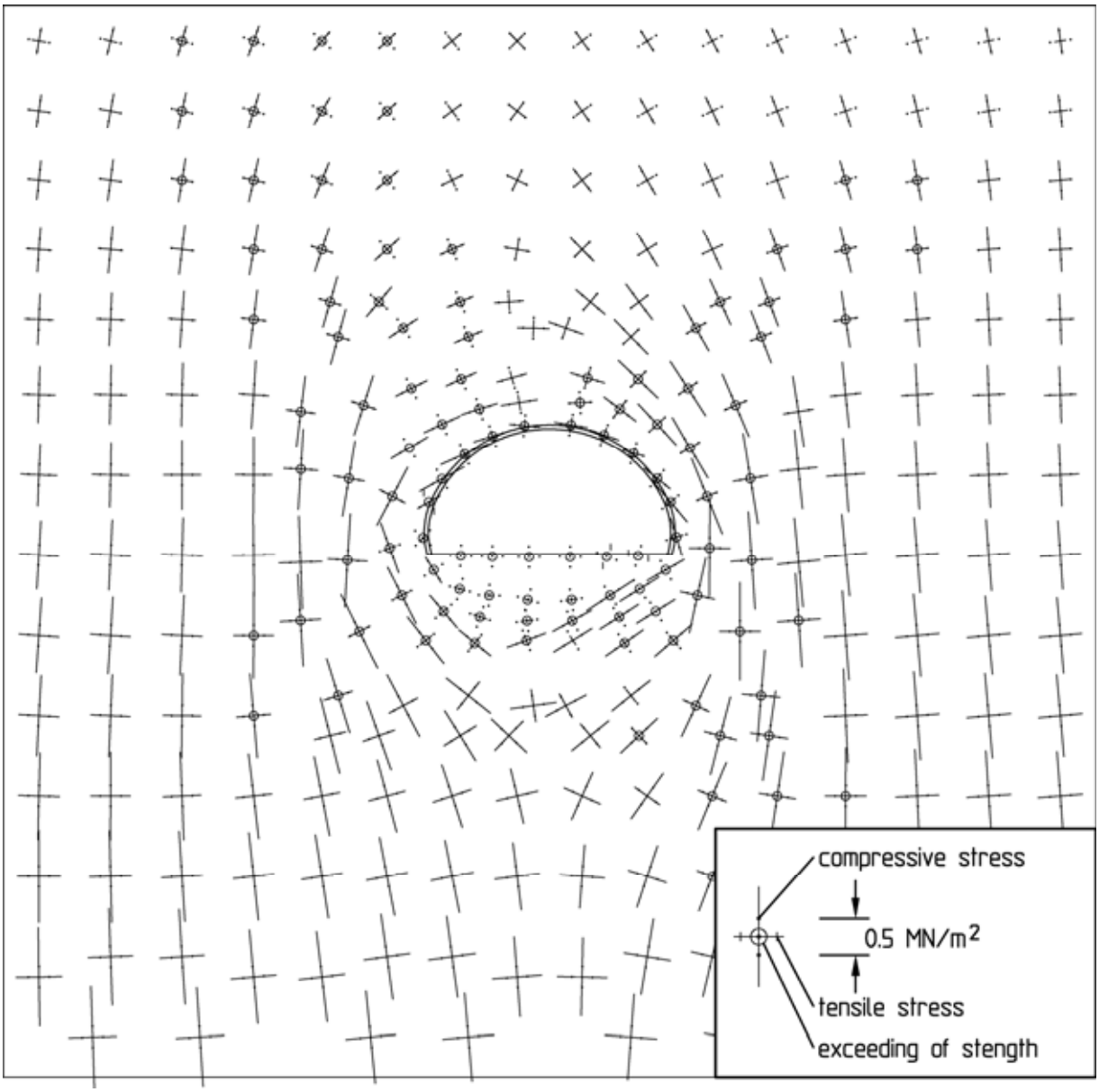

Fig. 3.12: Analysis cross-section AC 3 (structural model B), principal normal stresses and exceeding of strength, bench excavation (5th computation step)

If structural model C is assumed, the stability of the tunnel can be proven in the analysis for all construction stages even if the systematic anchoring is not taken into account. Also, if a greater

shear strength is assumed on the discontinuities, the computed displacements become considerably smaller.

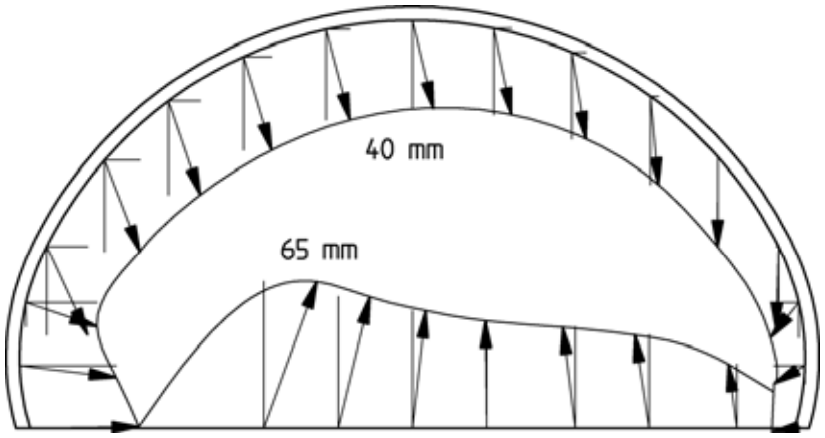

Fig. 3.13: Analysis cross-section AC 3 (structural model B), displacements, bench excavation (5^{th} – 1^{st} computation step)

Fig. 3.14 shows the bending moments and normal thrust in the shotcrete membrane calculated for the 5^{th} computation step. For a safety factor of 1.35, the design results in a statically required reinforcement of up to 4.0 cm^2/m. If the lattice girders are taken into account, this reinforcement is covered by the planned reinforcement (see Fig. 3.6).

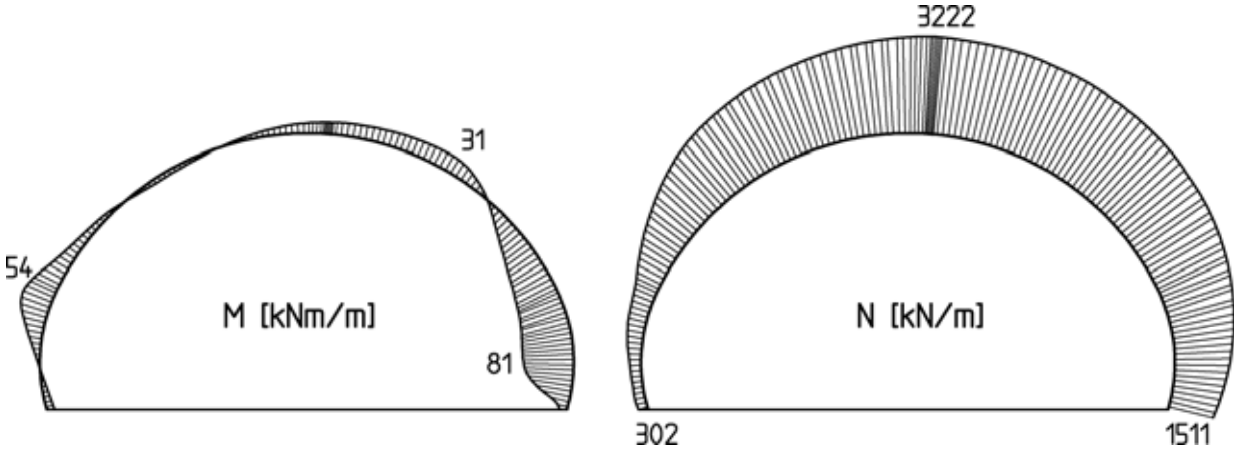

Fig. 3.14: Analysis cross-section AC 3 (structural model B), stress resultants in the shotcrete membrane, bench excavation (5^{th} computation step)

In Fig. 3.15 the tensile anchor forces computed for the truss elements for the 7^{th} computation step are shown. They reach a maximum value of approx. 130 kN.

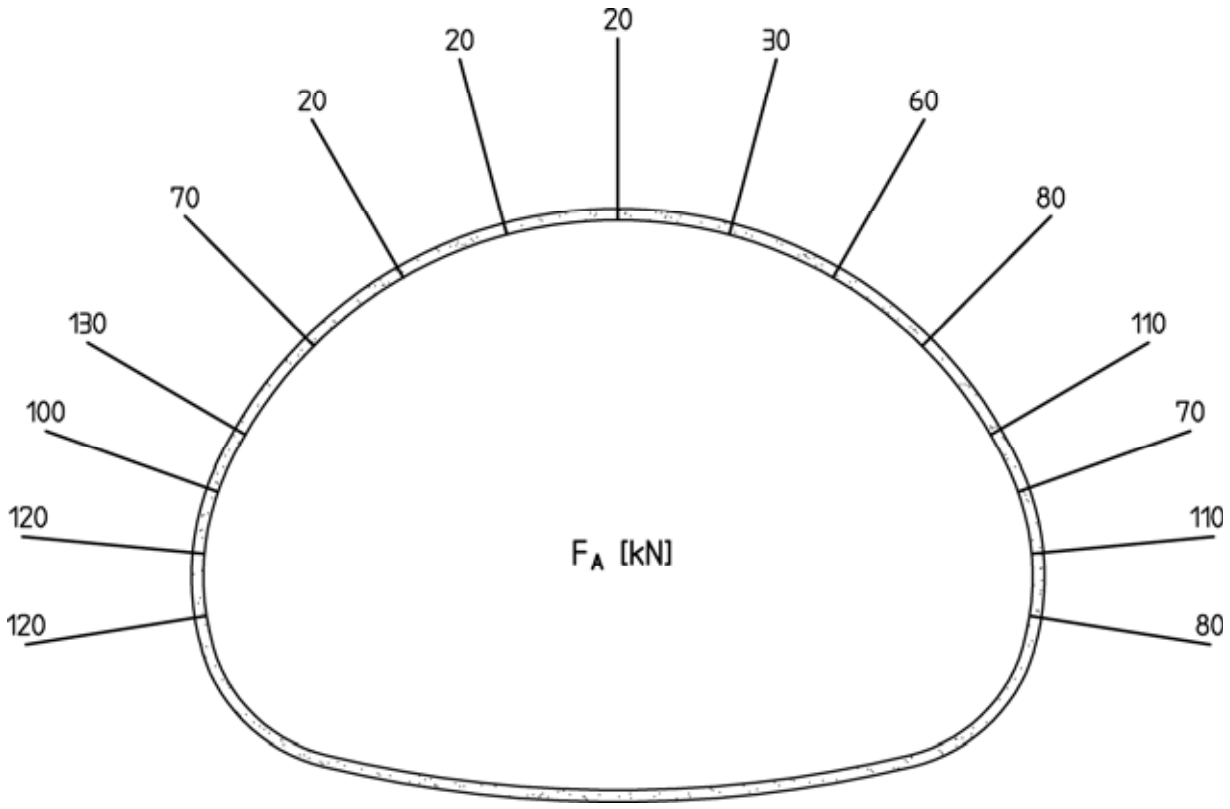

Fig. 3.15: Analysis cross-section AC 3 (structural model B), tensile anchor forces, 7th computation step

The admissable anchor force of the installed anchors adm F_A results from comparing the anchor force divided by the cross sectional area A_s with the tension yield point of the anchor steel β_s taking into account a factor of safety of η = 1.75. SN-anchors made from BSt 500S (β_s = 500 N/mm^2) with a diameter of 25 mm were selected (see Fig. 3.6). This leads to the admissable anchor force:

$$\text{adm } F_A = \frac{1}{\eta} \cdot \beta_s \cdot A_s = 140\,\text{kN} \qquad (3.1)$$

This value is not exceeded in the analysis (see Fig. 3.15).

With the computation of the anchor forces it must be taken into account that the placement of the anchors is simulated simultaneously with the excavation and the installation of the shotcrete membrane (see Fig. 3.11). Thus the anchor loads are overestimated in the analyses, since in reality the anchors are placed after the installation of the shotcrete membrane. To neutralize this effect, a Young's modulus smaller than the one of steel was assumed for the anchors in the analyses.

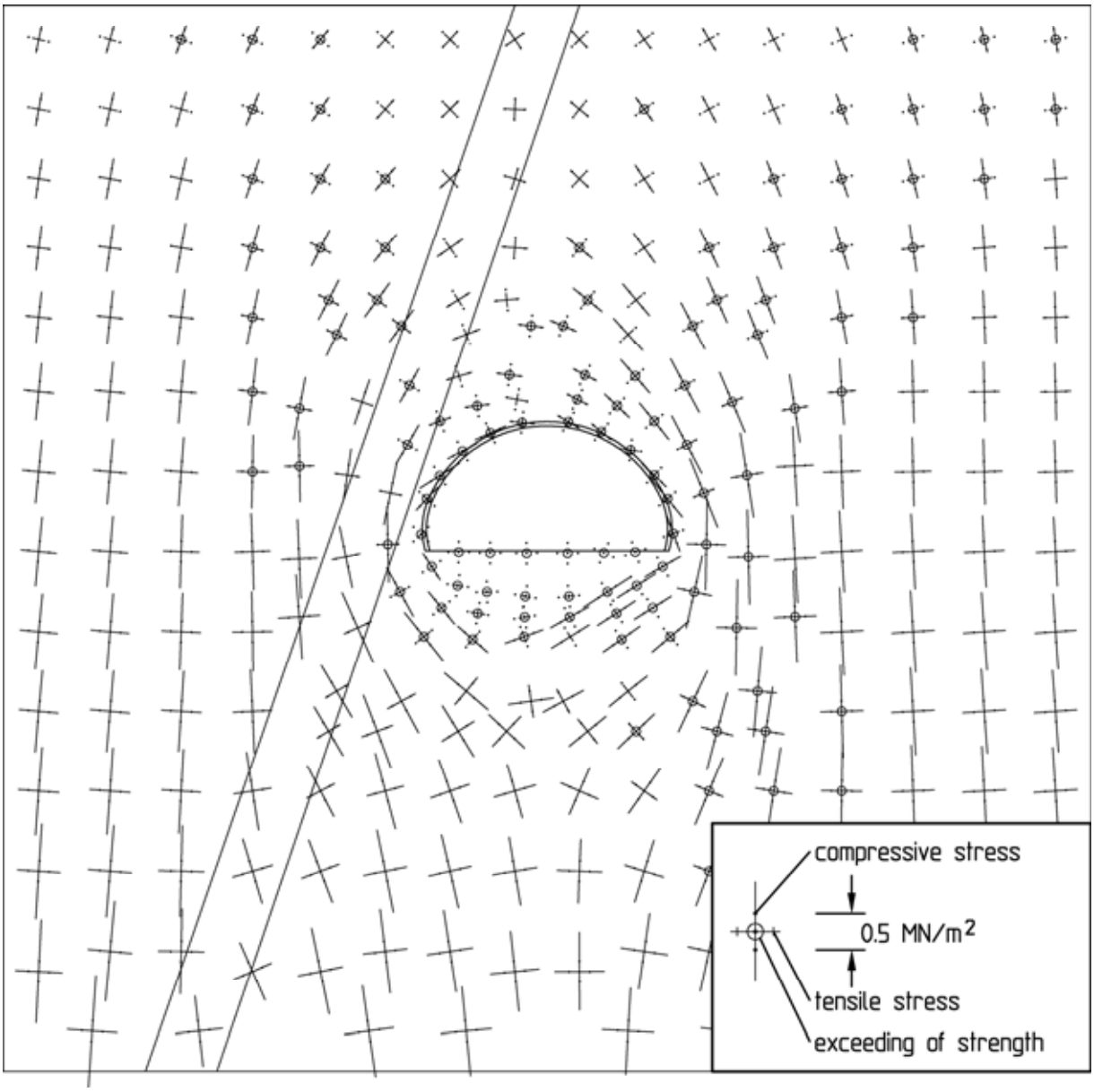

Fig. 3.16: Analysis cross-section AC 3 (structural model B), fault zone to the left of the tunnel, principal normal stresses and exceeding of strength, bench excavation (5^{th} computation step)

Due to the uncertainties involved with this approach regarding the computed anchor forces and stress resultants of the shotcrete membrane, a comparative analysis was carried out, in which the shear resistance of the anchors was converted into an equivalent cohesion on the discontinuities. This cohesion was assumed within the anchored area (see Chapter 2.3.2). The results of this analysis confirmed the reinforcement determined before and thus indirectly also the computed anchor forces.

Fig. 3.16 to 3.19 show the results of an analysis based on the parameters given in Fig. 3.9 and 3.10, structural model B and in addition a 5 m thick fault zone dipping at 70° close to the left side of the tunnel (see Fig. 3.8, position L). For these unfavorable assumptions the stability of the construction stage after the bench excavation (5th computation step, see Fig. 3.11) can only be proved in the analysis, if in the area of the left half of the tunnel 10 to 15 m long IBO-bolts (see Chapter 2.3.1) reaching behind the fault zone into the undisturbed rock mass are simulated by truss elements.

The principal normal stresses, the exceeding of strength and the displacements computed for this case for the 5th computation step are shown in Fig. 3.16 and 3.17. If the long anchors are simulated, the displacements of the excavation profile are of the same magnitude as for the corresponding case without a fault zone (see Fig. 3.13 and 3.17).

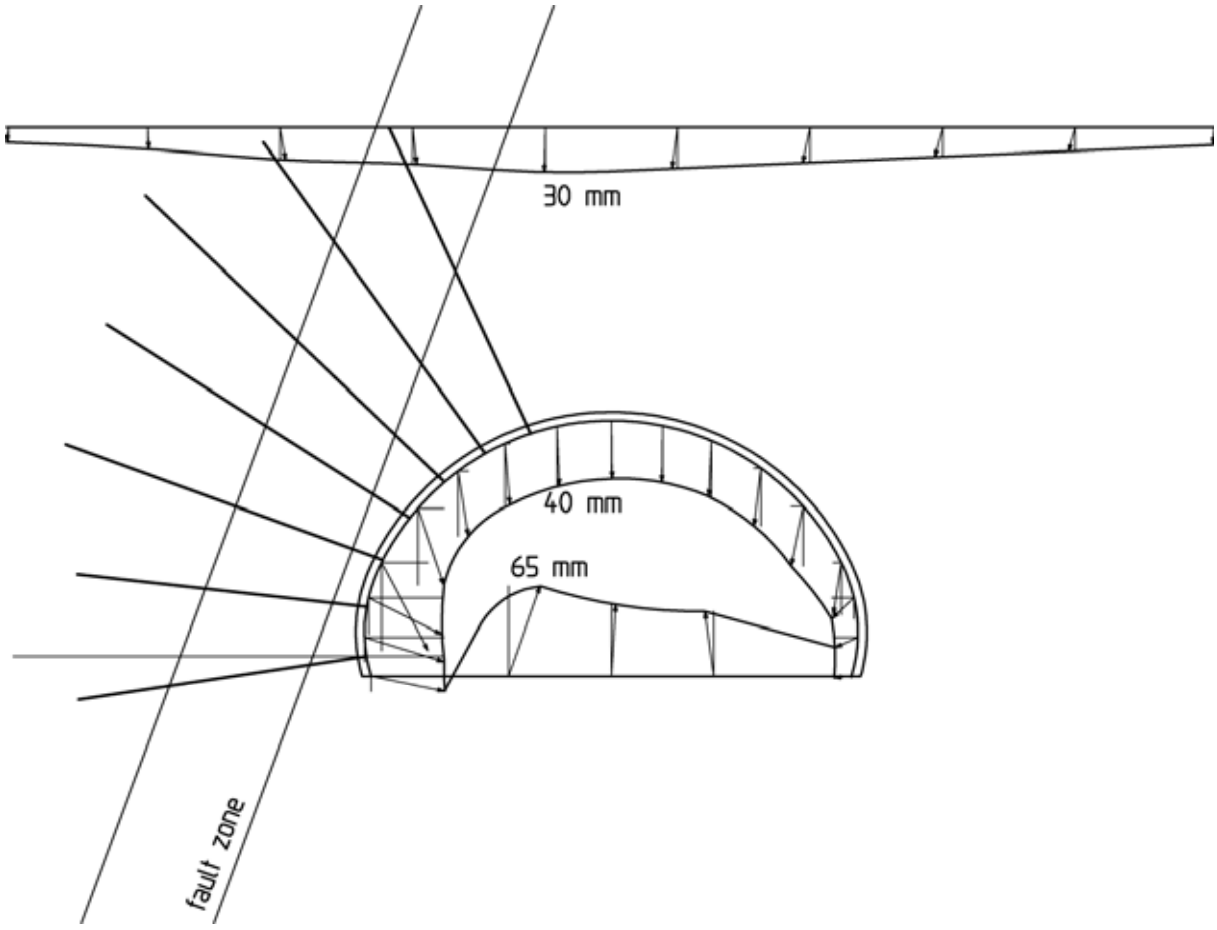

Fig. 3.17: Analysis cross-section AC 3 (structural model B), fault zone to the left of the tunnel, displacements, bench excavation (5th – 1st computation step)

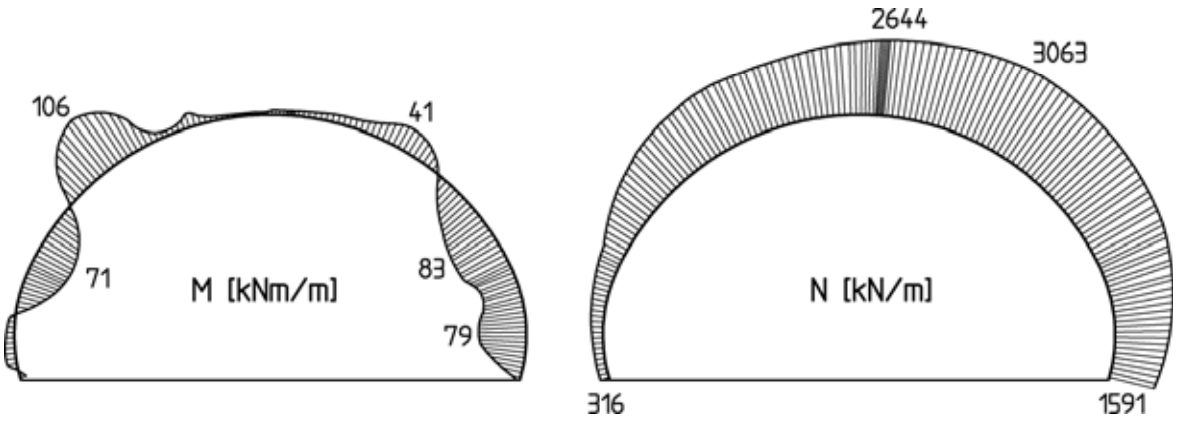

Fig. 3.18: Analysis cross-section AC 3 (structural model B), fault zone to the left of the tunnel, stress resultants of the shotcrete membrane, bench excavation (5th computation step)

Fig. 3.18 shows the bending moments and normal thrust in the shotcrete membrane determined for the 5th computation step. Compared to the corresponding case without a fault zone, greater maximum bending moments and smaller maximum normal thrusts occur in the shotcrete (see Fig. 3.14 and 3.18). For a safety factor of 1.35, the design results in a statically required reinforcement of up to 6.2 cm^2/m. If the lattice girders are taken into account, this reinforcement is covered by the planned reinforcement as well.

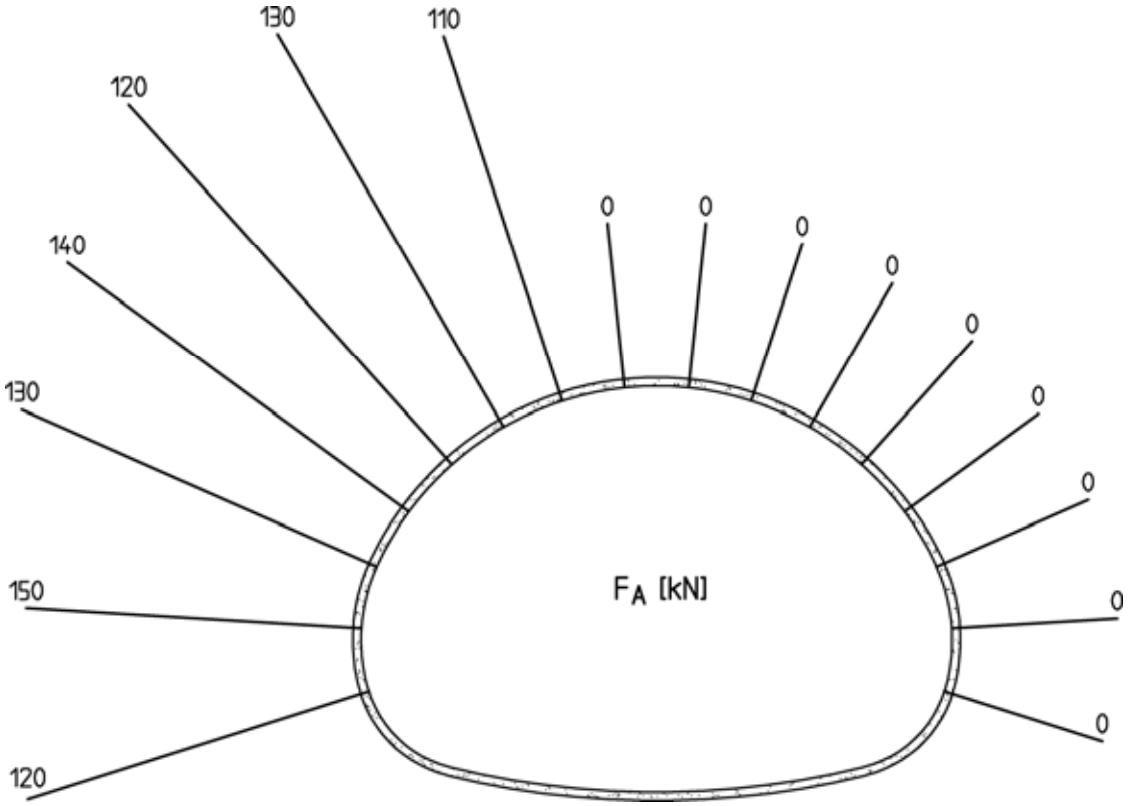

Fig. 3.19: Analysis cross-section AC 3 (structural model B), fault zone to the left of the tunnel, tensile anchor forces, 7th computation step

In Fig. 3.19 the tensile anchor forces computed for the truss elements in the 7th computation step are given. Only the anchors running through the fault zone are loaded. The maximum computed anchor force amounts to 150 kN, which is only slightly more than the admissible anchor load according to (3.1) of the planned IBO-rods (∅ 25 mm) of 140 kN.

3.1.6 Crown heading and monitoring results

Geotechnical mappings of the crown face were carried out in regular intervals during the heading. Special emphasis was placed on recording the properties, extent and orientation of the discontinuities (Fig. 3.20). No fault zones were encountered in the tunnel cross-section.

Further, in the area of tunnel cross-section TC 3 ca. 20 measuring cross-sections with gage bolts were installed to monitor the displacements caused by the heading. In tunnel cross-sections TC 1 and TC 2 further measuring cross-sections were installed.

As already mentioned, the excavation classes were determined on the basis of the results of the stability analyses as well as the mappings and the displacement measurements. Fig. 3.21 shows exemplarily the maximum roof subsidence measured during crown heading in the area of tunnel cross-sections TC 3 and TC 3A. With the exception of one measurement in the portal area (δ_R = 16 mm), the measured values range from 1 to 7 mm.

In the area of the three analysis cross-sections AC 1, AC 2 and AC 3, the measured roof subsidence can be compared with the results of the stability analyses. With this comparison it must be taken into account, however, that the displacements that occurred in the measuring cross-sections already before the zero reading cannot be measured. Since the elastic part of the displacements mostly occurred before the zero reading, the measured roof subsidence δ_R can approximately be compared with the viscoplastic part of the displacements computed for the roof δ_R^{vp}. It becomes apparent that in the area of analysis cross-sections AC 2 and AC 3 the measured displacements are smaller than the viscoplastic parts of the displacements computed with no cohesion assumed on the foliation-parallel discontinuities (c_f = 0, see Fig. 3.9).

a

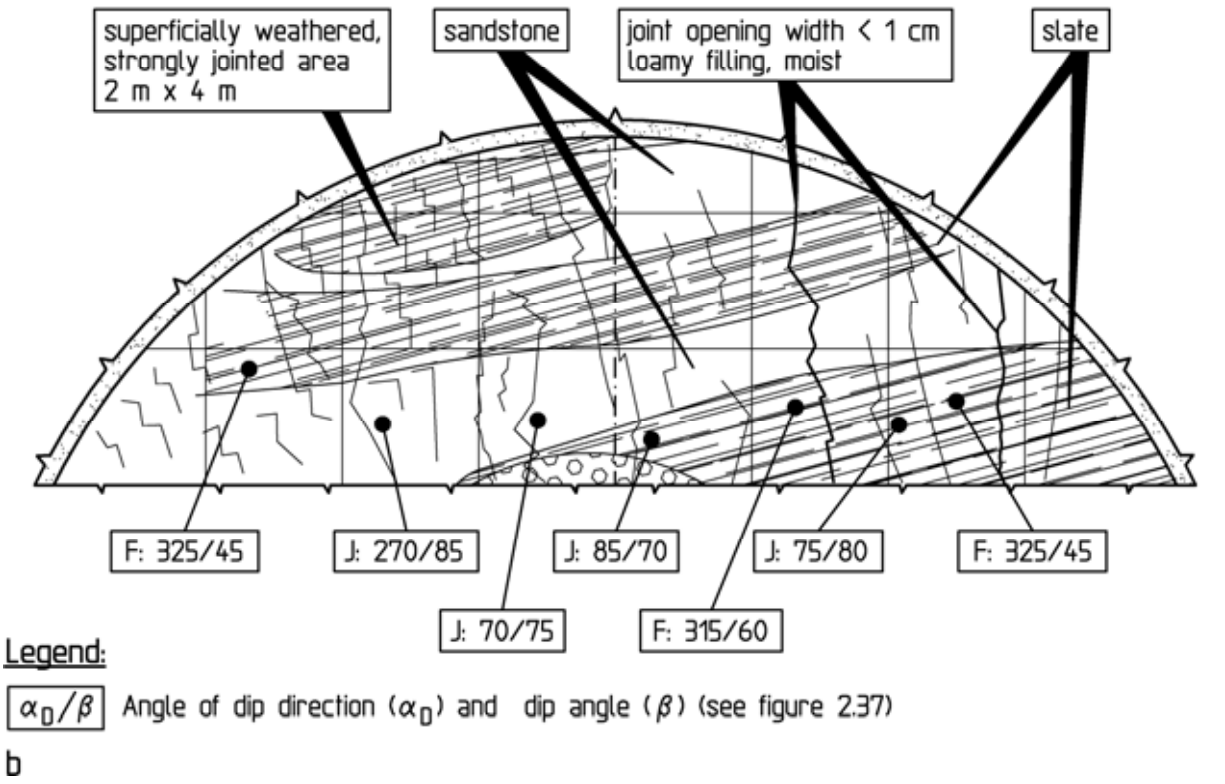

b

Fig. 3.20: Crown face, chainage 216.1 m, excavation class 5: a) Photograph; b) mapping

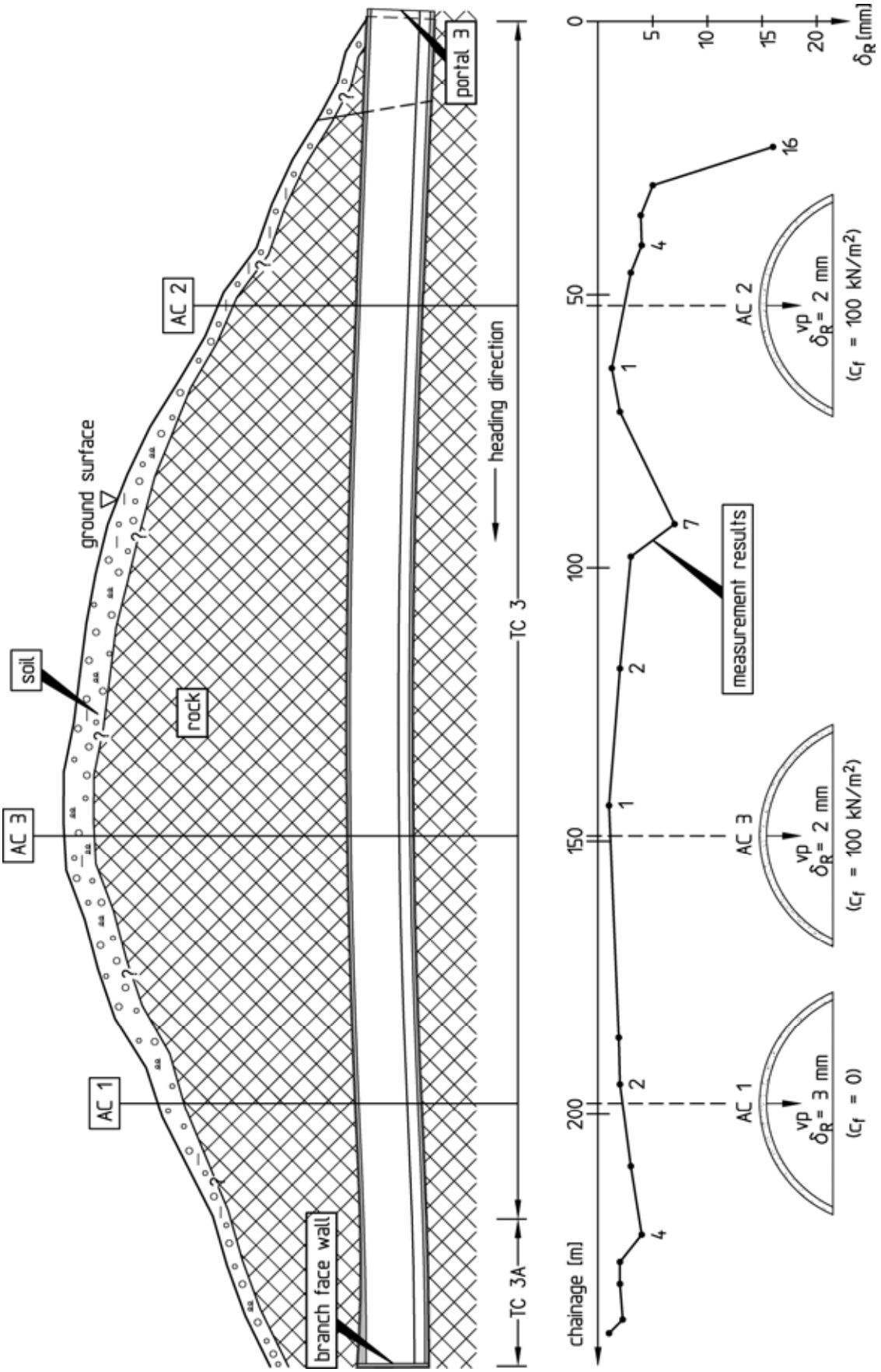

Fig. 3.21: Crown heading, comparison of measured and computed roof subsidence, tunnel cross-sections TC 3 and TC 3A

If a value of c_f = 100 kN/m^2 is chosen for the cohesion on the foliation parallel discontinuities, the measured roof subsidence corresponds to the computed viscoplastic part of the displacements. For analysis cross-section AC 1, c_f = 0 yields good agreement of the measured roof subsidence with the computed viscoplastic part of the displacements (Fig. 3.21).

The results of the geotechnical mapping of the tunnel face and the displacements measured during the crown heading allowed in consideration of the results of the stability analyses the tunnel to be driven with excavation classes 4, 5 and 6A (see Fig. 3.6). Excavation class 7A was not carried out. Further, it was possible to excavate the crown over the entire tunnel length without simultaneously trailing bench.

3.1.7 Conclusions

The Glockenberg Tunnel is located in an alternating sequence of slates and sandstones characterized by a tectonic deformation due to a "special folding". The strength and deformability of the rock mass is predominantly determined by the discontinuities (bedding parallel discontinuities, foliation parallel discontinuities and joints). As a consequence of the folding structure, the orientation of the discontinuities is not uniform. In addition, the strike directions of the discontinuities with respect to the tunnel axis vary due to the almost circular tunnel alignment. Fault zones had to be expected locally as well.

Therefore, different structural models had to be assumed for the stability analyses. The comparison of the displacements measured during tunneling with the values computed for the different cases allowed to optimize the support measures and to apply economical excavation classes. It became apparent that the analyses represented an essential contribution to an economical construction of this tunnel.

3.2 Gäubahn Tunnel in Stuttgart, Germany

3.2.1 Introduction

The Gäubahn Tunnel is part of the new construction of the federal highway B 14 between the Schattenring intersection and the Südheimer Square providing a northern bypass of the city district of Vaihingen in Stuttgart, Germany. It undercrosses a railway line (Gäubahn) and buildings adjacent to the Rudolf-Sophien institution. During the heading underneath the railway track railway traffic had to be maintained. Specific tunnel support measures were therefore planned for this section.

3.2.2 Structure

The Gäubahn Tunnel consists of two parallel ca. 300 m long tunnel tubes with two lanes each (Fig. 3.22). Approx. 270 m of each tunnel tube were driven by underground construction ascending from the eastern portal. The precuts in the portal areas were constructed by the cut-and-cover method (Fig. 3.22 and 3.23).

The maximum overburden amounts to approx. 20 m. In the area of the undercrossing of the Gäubahn an overburden of approx. 4 m exists (Fig. 3.23).

Fig. 3.24 shows the 11.5 m wide and 8.85 m high standard profile of a tunnel tube. The excavated cross-section amounts to approx. 93 m^2. The shotcrete membrane has a concrete grade of B25 and a thickness of 25 to 30 cm. The interior lining consists of watertight grade B35 concrete with a thickness of 45 cm.

The roof and the invert are shallowly rounded with radii of curvature of R = 8.15 m and R = 10.45 m, respectively. At the sidewalls the radius of curvature amounts to R = 5.45 m. The transitions from the sidewalls to the roof and to the invert, respectively, were designed with comparatively small radii of R = 3.06 m and R = 2.65 m, respectively (Fig. 3.24).

The two tunnel tubes were constructed by advancing crown heading with trailing bench and invert excavation. The cross-section is correspondingly divided into crown and bench/invert (Fig. 3.24).

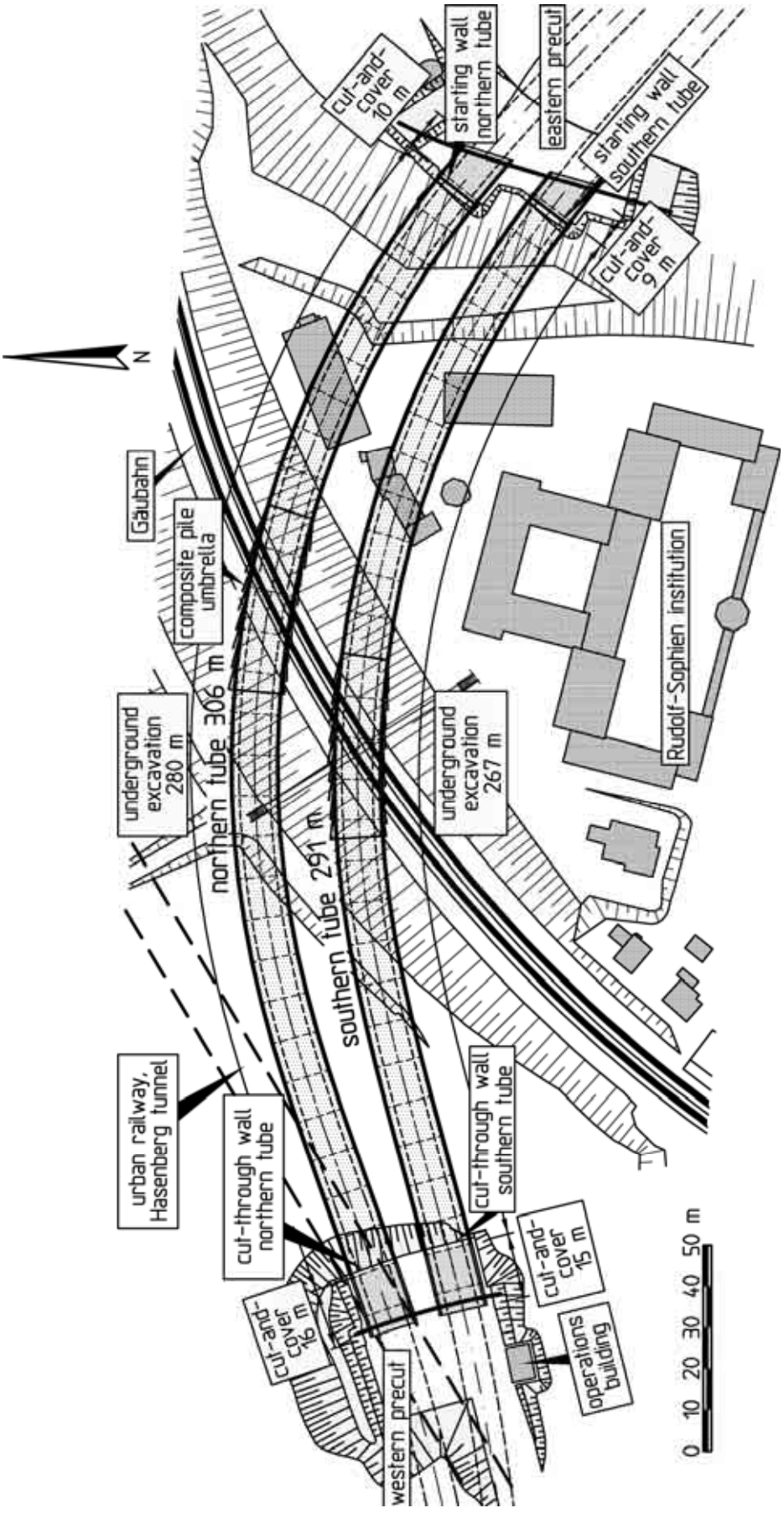

Fig. 3.22: Gäubahn Tunnel, site plan

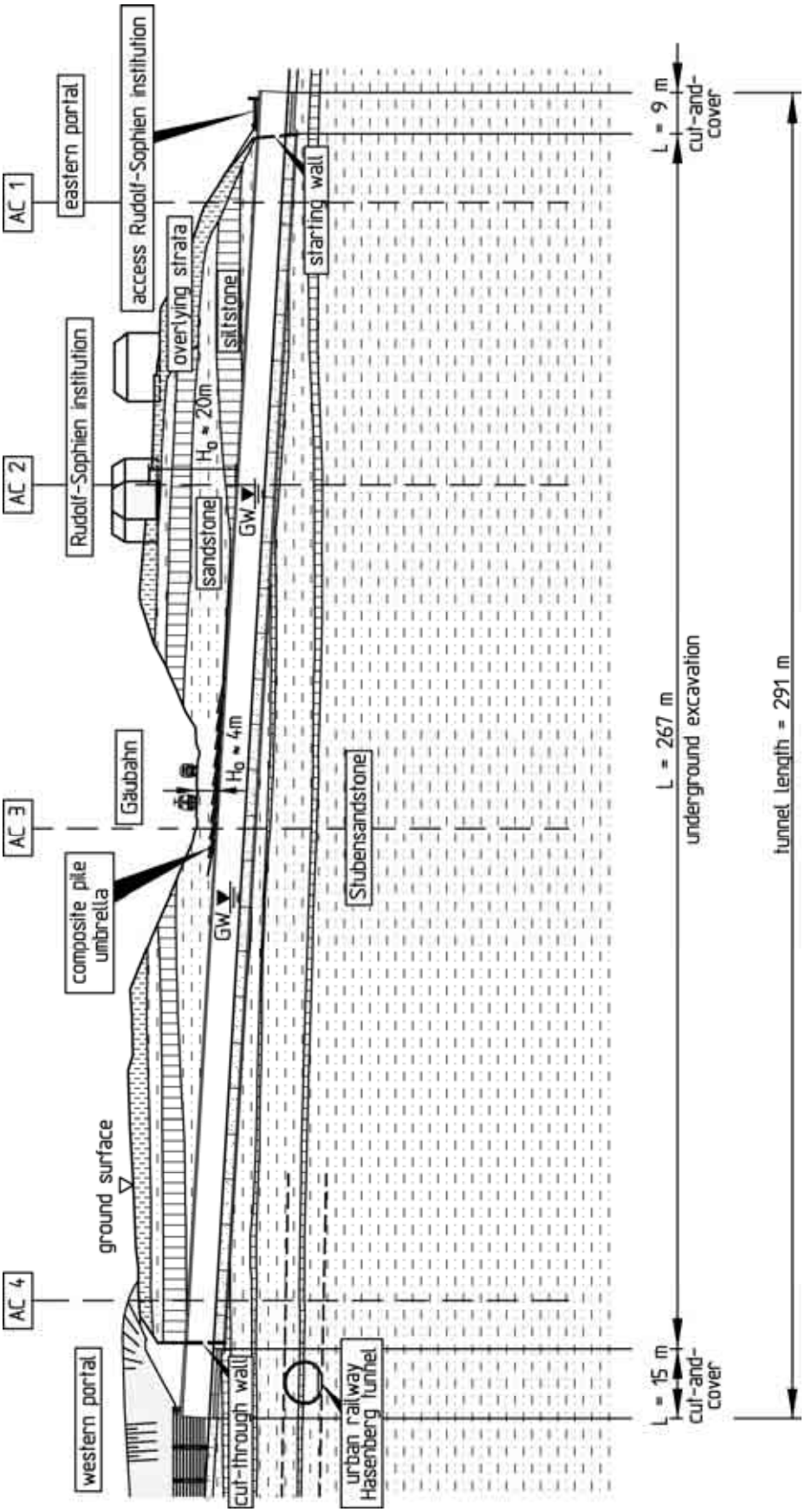

Fig. 3.23: Gäubahn Tunnel, longitudinal section through the southern tube with ground profile and analysis cross-sections

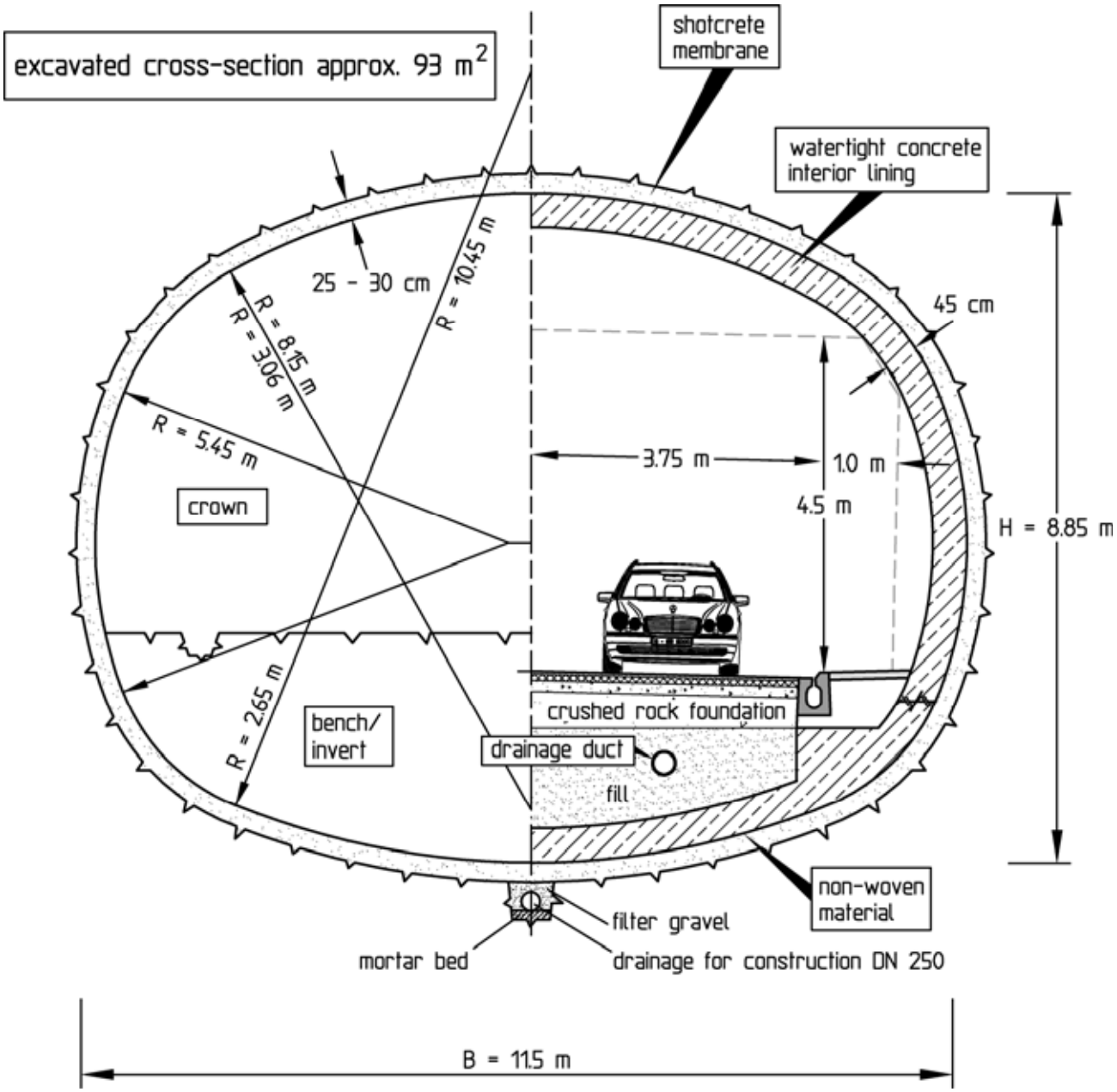

Fig. 3.24: Gäubahn Tunnel, standard profile

Fig. 3.25 is an aerial photograph of the eastern precut with the buildings of the Rudolf-Sophien institution after the excavation and support of both tunnel tubes. The picture shows the open-cut arch sections (cut-and-cover construction) in the transition from underground excavation to the portal blocks not yet built in the represented construction phase.

Fig. 3.25: Gäubahn Tunnel, eastern precut and Rudolf-Sophien institution

3.2.3 Ground and groundwater conditions

Below the ground surface a few meters thick overlying strata are present (Fig. 3.23). They consist mostly of rock weathered into sand and silt, respectively, and partially relocated.

The rock mass underneath belongs stratigraphically to the Stuben-sandstone formation consisting of a sequence of sandstones and siltstones. The sandstone and siltstone layers are up to several meters thick. Locally, however, also narrowly spaced alternating sequences occur (Fig. 3.23).

The sandstones as well as the siltstones are divided into banks by bedding planes. The thickness of these banks ranges between few centimeters and 1 to 2 m. The bedding planes are approximately horizontal.

The joints are generally steeply dipping and deviate only little from the direction perpendicular to the bedding (here: the vertical direction). In general they extend over many meters horizon-

tally. At least in some areas the joints are slightly opened according to the exploration results.

In the siltstone layers slickensides were found as well in addition to the bedding planes and joints. These slickensides are randomly oriented and have mostly smooth surfaces.

In the middle tunnel section two boreholes were equipped as observation wells. According to their readings, the groundwater table was located at the level of the two tunnel cross-sections (Fig. 3.23). In two observation wells located close to the tunnel portals no groundwater was encountered.

3.2.4 Excavation classes

The excavation of the two tunnel tubes was planned mostly as an advancing crown heading with open invert and trailing bench and invert excavation following excavation class 4A.

The excavation sequence, excavation method, round lengths and support measures for excavation classes 4A-1, 4A-2 and 4A-3 (see DGGT, 1995: Table 1) are given in Fig. 3.26. These excavation classes differ with regard to in the unsupported round length, the lattice girder spacing and the number of anchors per round. The shotcrete membrane is reinforced inside and outside with steel fabric mats Q295. If necessary, the tunnel face was planned to be sealed with plain shotcrete. The trailing distance of bench (D) and invert (E) was to be determined depending on the monitoring results and the geotechnical conditions encountered during the heading as well as depending on the results of the stability analyses.

The tunnel was excavated using a tunnel excavator and, in some areas, also by smooth blasting. Measurements carried out on buildings showed that the vibration velocities remained far under the reference values for the admissible structural vibrations given in DIN 4150, part 3 (DIN 4150-3, 1999).

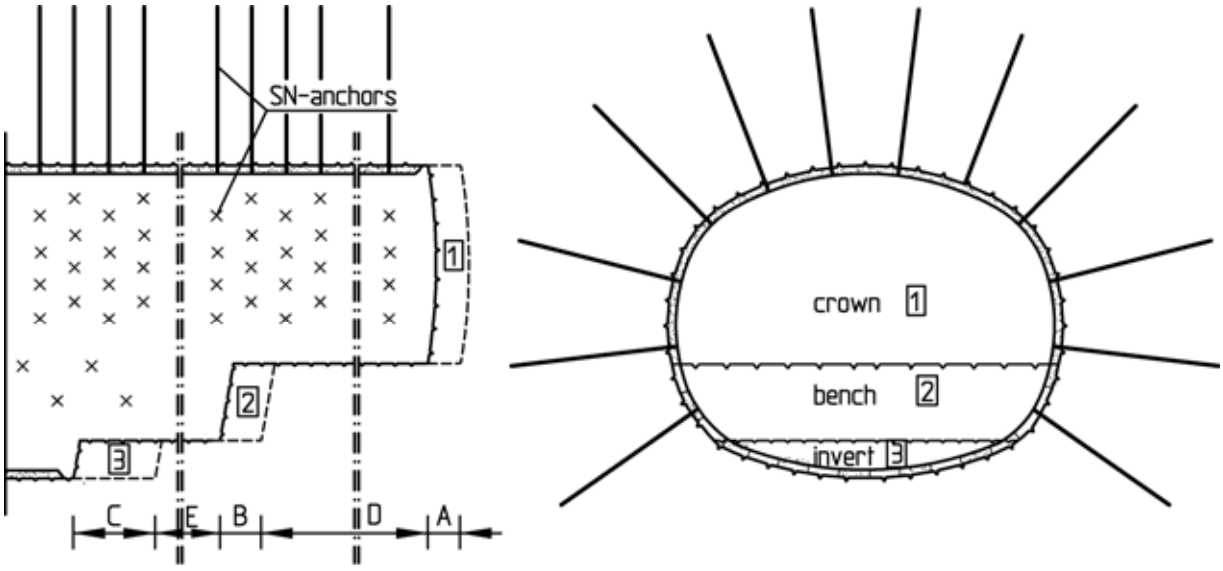

excavation class		4A-1	4A-2	4A-3
excavation method		smooth blasting/ mechanical excavation		
unsupported round length	crown (A) bench (B) invert (C)	0.80 - 1.20 m 1 mat width 2 mat widths	1.21 - 1.60 m 1 mat width 2 mat widths	1.61 - 2.00 m 1 mat width 2 mat widths
shotcrete B25		t = 25 cm	t = 25 cm	t = 25 cm
reinforcement		steel fabric mats Q 295 (2 layers)	steel fabric mats Q 295 (2 layers)	steel fabric mats Q 295 (2 layers)
lattice girder spacing	crown	0.80-1.20 m	1.21-1.60 m	1.61-2.00 m
systematic anchoring, BSt 500 S (ca. 1 anchor/2-3 m^2)		SN Φ 25 L_A = 4-6 m 11 - 12 pcs./round	SN Φ 25 L_A = 4-6 m 13 - 14 pcs./round	SN Φ 25 L_A = 4-6 m 15 - 16 pcs./round
tunnel face sealing		shotcrete 3 cm (if required; on parts of the face only)		
advance support		none		
trailing distance	bench (D) invert (E)	depending on the monitoring results, the geotechnical conditions encountered during the heading and on the results of stability analyses		

Fig. 3.26: Standard heading, excavation classes 4A-1, 4A-2 and 4A-3

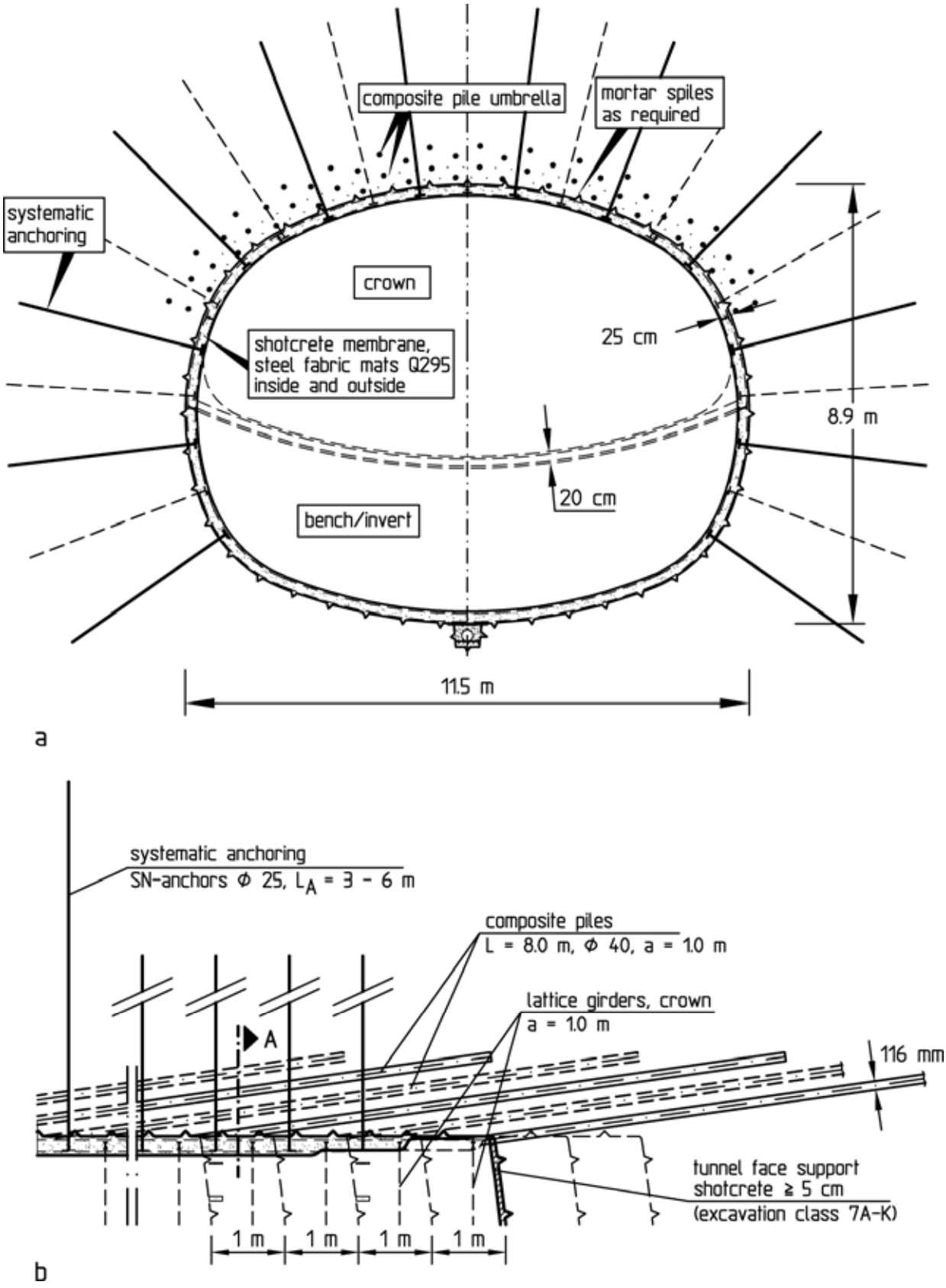

Fig. 3.27: Undercrossing of the Gäubahn, excavation classes 6A-K and 7A-K: a) Cross-section; b) longitudinal section (detail)

In the area of the undercrossing of the Gäubahn a crown heading with closed temporary invert with the excavation classes 6A-K and 7A-K, respectively, was planned (see DGGT, 1995: Table 1) in order to limit the tunneling-induced subsidence (Fig. 3.27). These excavation classes include an advancing support using so-called composite pile umbrellas. These consist of 8 m long piles with a diameter of 40 mm which were grouted in 116 mm boreholes using cement based suspension and are slightly inclined against the horizontal in the longitudinal section (Fig. 3.23 and 3.27). In each round one layer of composite piles (composite pile umbrella) was constructed. If required, spiles were planned to be installed in addition. In excavation class 7A-K, the tunnel face was in addition to be rounded out and supported with shotcrete (Fig. 3.27b).

3.2.5 Stability analyses for the design of the shotcrete support

For the design of the shotcrete membrane, two-dimensional analyses with the program system FEST03 (Wittke, 2000) were carried out.

The investigation comprised the analysis cross-sections AC 1 to AC 4 shown in Fig. 3.23. Fig. 3.28 shows exemplarily the FE-mesh, the boundary conditions, the ground profile and the parameters used for analysis cross-section AC 2. Analysis cross-section AC 2 is located in the area of the undercrossing of the buildings adjacent to the Rudolf-Sophien institution. The overburden in this area amounts to approx. 20 m (see Fig. 3.23).

The 52 m wide, 66 m high and 1 m thick computation section in the form of a slice is discretized by an FE-mesh with 2703 isoparametric elements and 13956 nodes. To simplify matters, only one tunnel tube is modeled. The plane of symmetry lies in the middle of the rock pillar between the two tunnel tubes. Thus the simultaneous excavation of both tunnel tubes is simulated in the analyses. In reality, the crown excavation of one tunnel tube precedes the other one. The simulation of a simultaneous heading of both tubes however is on the safe side with regard to the loading of the rock mass and the stability of the openings. For the nodes of the vertical boundary planes vertically movable supports are introduced as boundary conditions, whereas for the nodes on the lower boundary plane (z = 0) horizontally movable supports are specified (Fig. 3.28). All nodes are fixed in the y-direction.

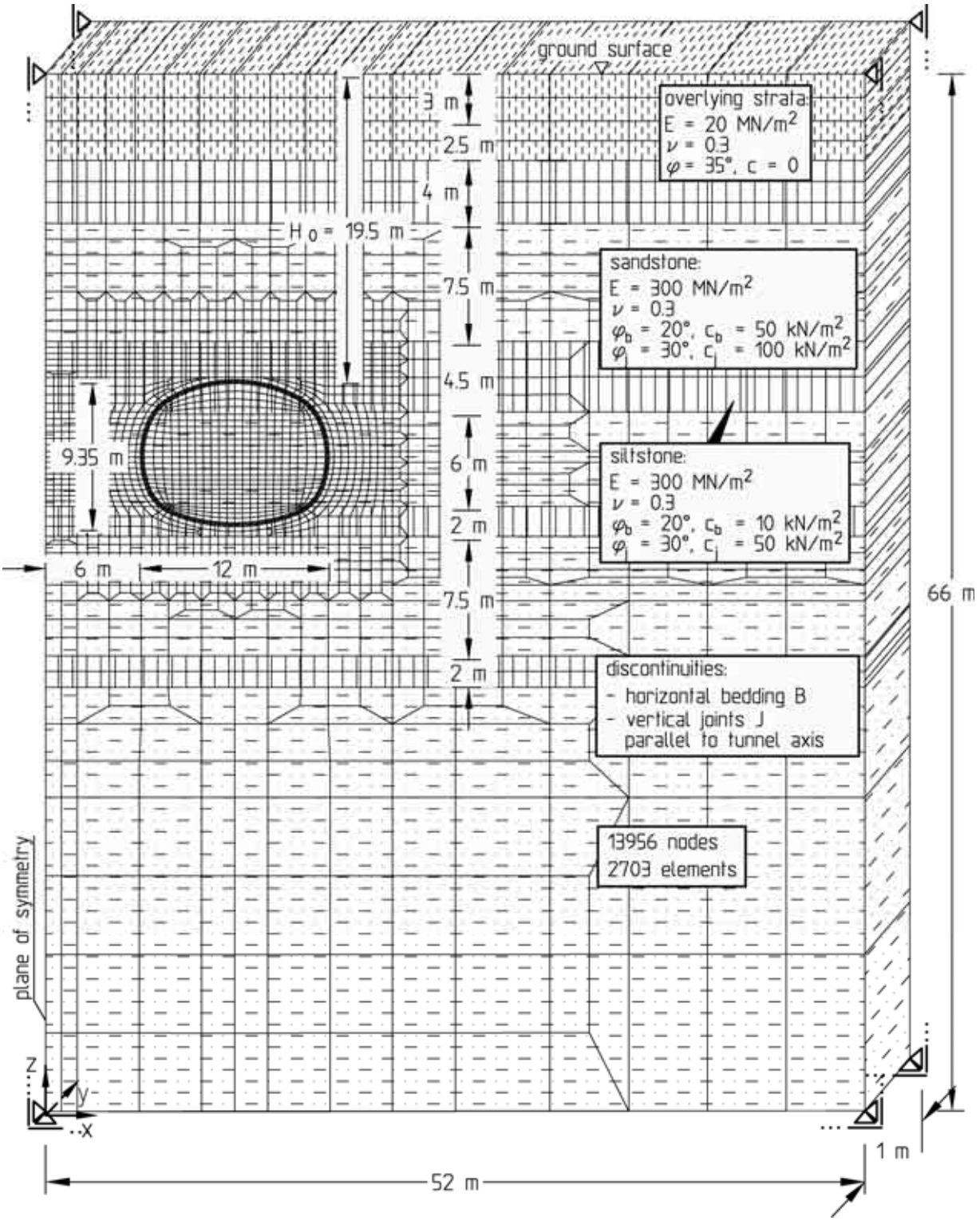

Fig. 3.28: Analysis cross-section AC 2, FE-mesh, boundary conditions, ground profile and parameters

Four sandstone and siltstone horizons each of the alternating sequence of the Stubensandstone formation were modeled. The positioning of the siltstone horizon in the roof area is to be assessed unfavorable with respect to the stability of the tunnel,

since the strength of the discontinuities is considered smaller in the siltstone than in the sandstone (see Fig. 3.28). At middle tunnel level a sandstone layer is modeled which is followed by a siltstone layer in the area of the tunnel invert. The groundwater table was assumed at tunnel invert level due to the drainage during construction. Below the groundwater table the rock mass is subjected to hydrostatic uplift.

In the tender documents ranges for the soil and rock mechanical parameters are given. The stability analyses for the design of the shotcrete support are based on the most unfavorable values (Fig. 3.28).

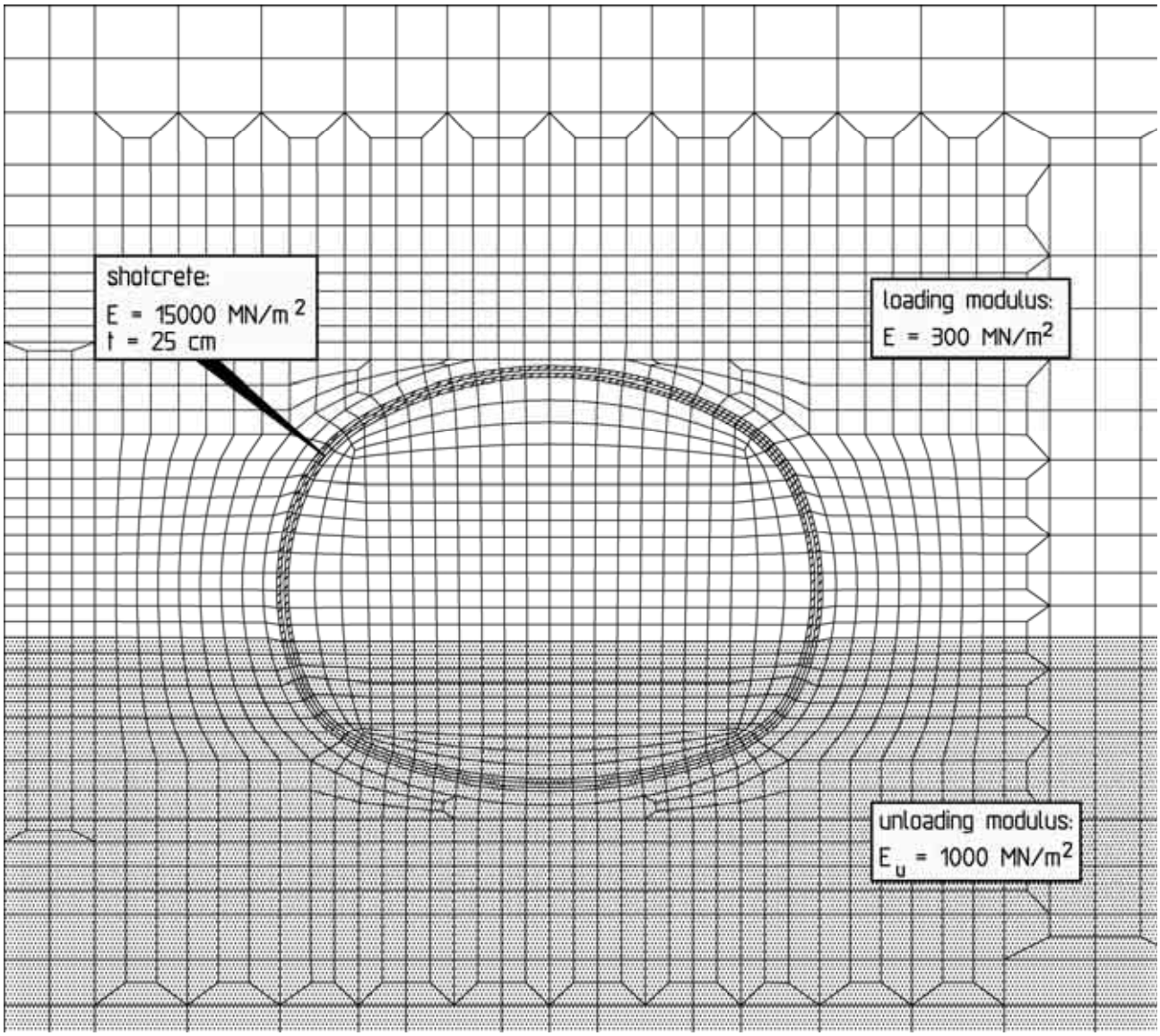

Fig. 3.29: Analysis cross-section AC 2, FE-mesh, detail

The intact rock strength of the sand- and siltstones was assumed infinitely high as a simplification. The rock matrix was assigned elastic stress-deformation behavior. This simplification is justified, because the strength on the discontinuities is markedly smaller than the intact rock strength. Two discontinuity sets were taken into account in the analyses. The horizontal bedding and a vertical joint set striking parallel to the tunnel axis with an unfavorable effect on tunnel stability.

At and underneath the tunnel invert, the rock mass is unloaded during the tunnel excavation. Previous experience has shown that the modulus relevant for the unloading of the rock mass is higher than the loading modulus assumed as E = 300 MN/m^2. Correspondingly, the elements in and underneath the invert area were assigned an unloading modulus of E_U = 1000 MN/m^2 (see Fig. 3.29).

The statically effective Young's modulus of the shotcrete was specified as 15000 MN/m^2 taking into account the hardening during the application of the load (Fig. 3.29).

The excavation and support of the tunnel were simulated in five computation steps (Fig. 3.30). The first computation step comprises the determination of the state of stress and deformation resulting from the dead weight of the ground (in-situ state). With computation steps 2 and 3 the crown excavation and its support using shotcrete are simulated. To this end, Young's modulus of the elements in the crown was reduced in the 2nd computation step to the value $E_{red} = a_v \cdot E$ with $a_v = 0.5$. a_v is the so-called stress relief factor already mentioned in Chapter 3.1 (Wittke, 2000). The excavation and support of the crown follow in the 3rd computation step. In the 4th and 5th computation steps the excavation and support of the remaining cross-section are simulated correspondingly.

Fig. 3.31 shows the displacements due to the crown excavation (3rd – 1st computation step) calculated for the excavation contour and the ground surface. The roof subsidence amounts to approx. 18 mm, the invert heave is approx. 8 mm and the maximum subsidence at the ground surface results to approx. 11 mm.

1st computation step:
state of stress and deformation resulting from the dead weight of the ground (in-situ state)

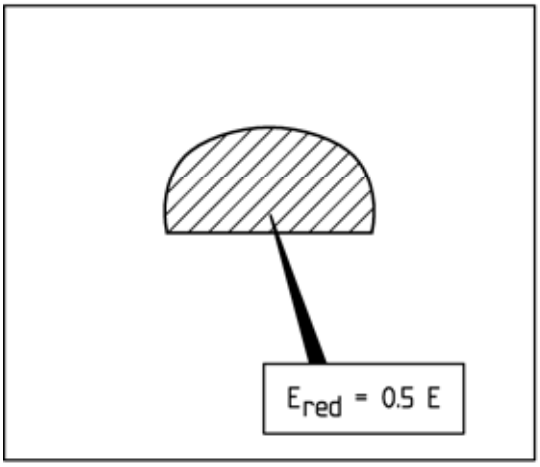

2nd computation step:
preceding stress relief in the crown

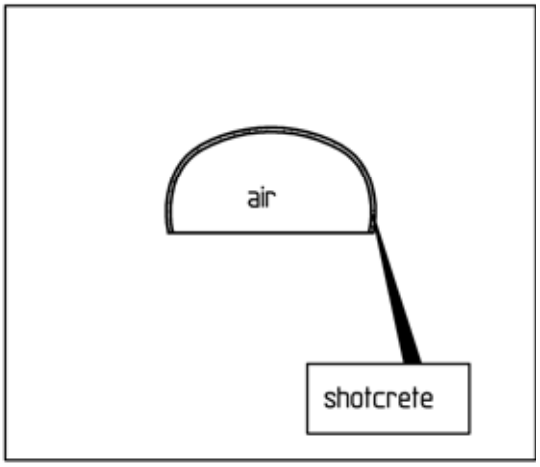

3rd computation step:
crown excavation and support

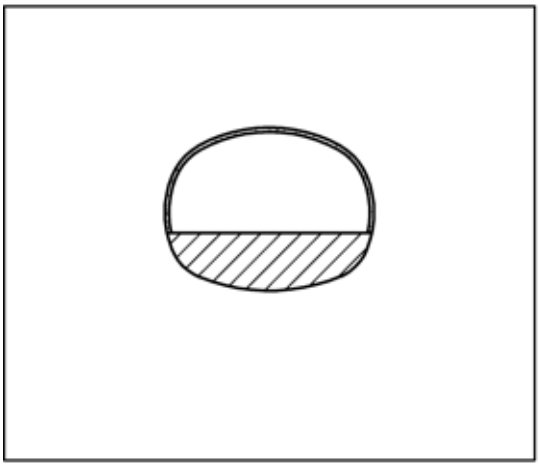

4th computation step:
preceding stress relief in the bench/invert

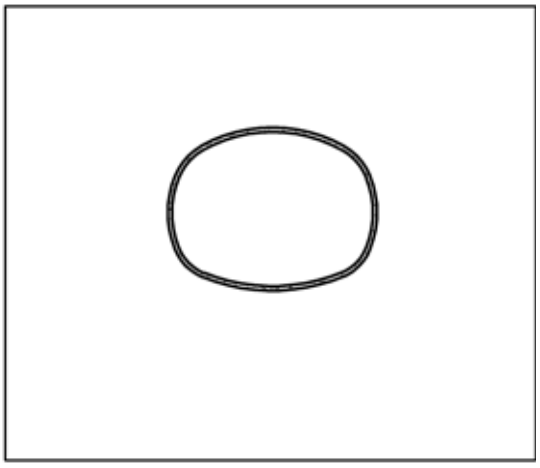

5th computation step:
bench/invert excavation and support

Fig. 3.30: Analysis cross-section AC 2, computation steps

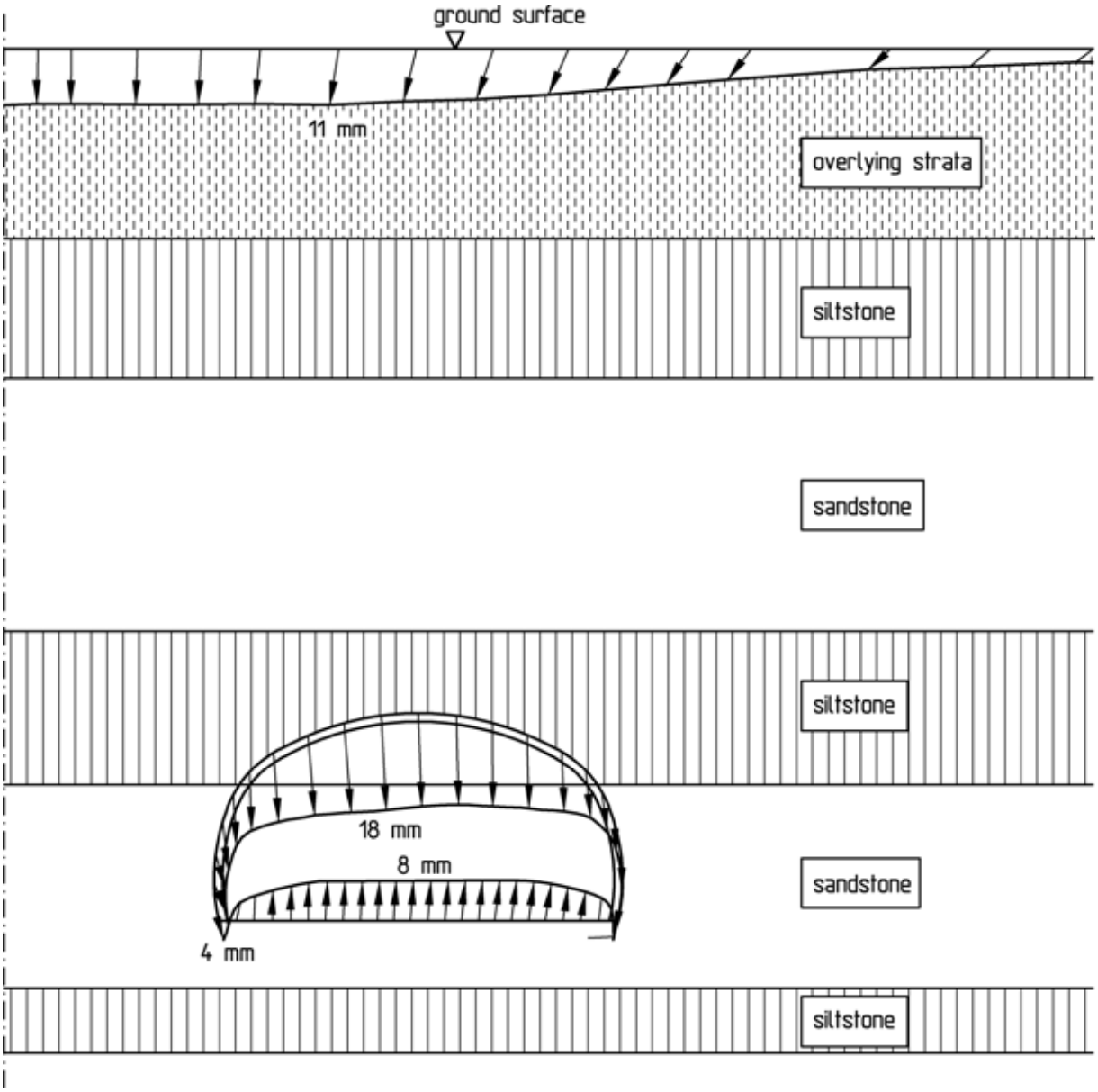

Fig. 3.31: Analysis cross-section AC 2, displacements, crown excavation (3rd – 1st computation step)

The computed bending moments and normal thrust in the shotcrete membrane are shown for the 3rd computation step in Fig. 3.32. The design of the shotcrete support for this construction stage yields that no reinforcement is required with respect to bending and normal thrust for a factor of safety of 1.35. Steel fabric mats Q295 were placed inside and outside as a minimum reinforcement (see Fig. 3.26).

After the bench and invert excavation in the 5th computation step the displacements increase only slightly. For this construction stage as well, no reinforcement is statically required for a factor of safety of 1.35.

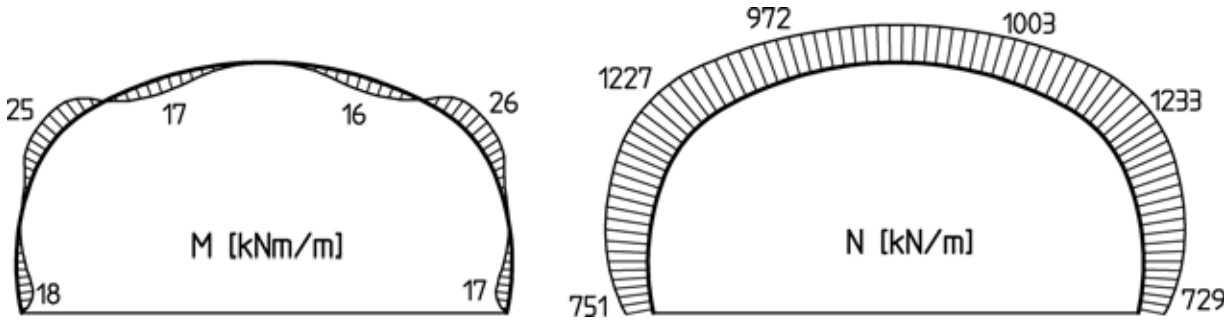

Fig. 3.32: Analysis cross-section AC 2, stress resultants in the shotcrete membrane, crown heading (3rd computation step)

3.2.6 Crown heading and monitoring results

To monitor the stability and to verify the results of the stability analyses the heading was accompanied by a geotechnical monitoring program.

The following measurements were carried out:

- Leveling and trigonometric measurements on the ground surface,
- leveling on structures,
- leveling on sleepers of the Gäubahn,
- trigonometric measurements on overhead wire poles,
- combined extensometer and inclinometer measurements in the area of the undercrossing of the Gäubahn and at the western portal,
- leveling and convergency measurements in both tunnel tubes.

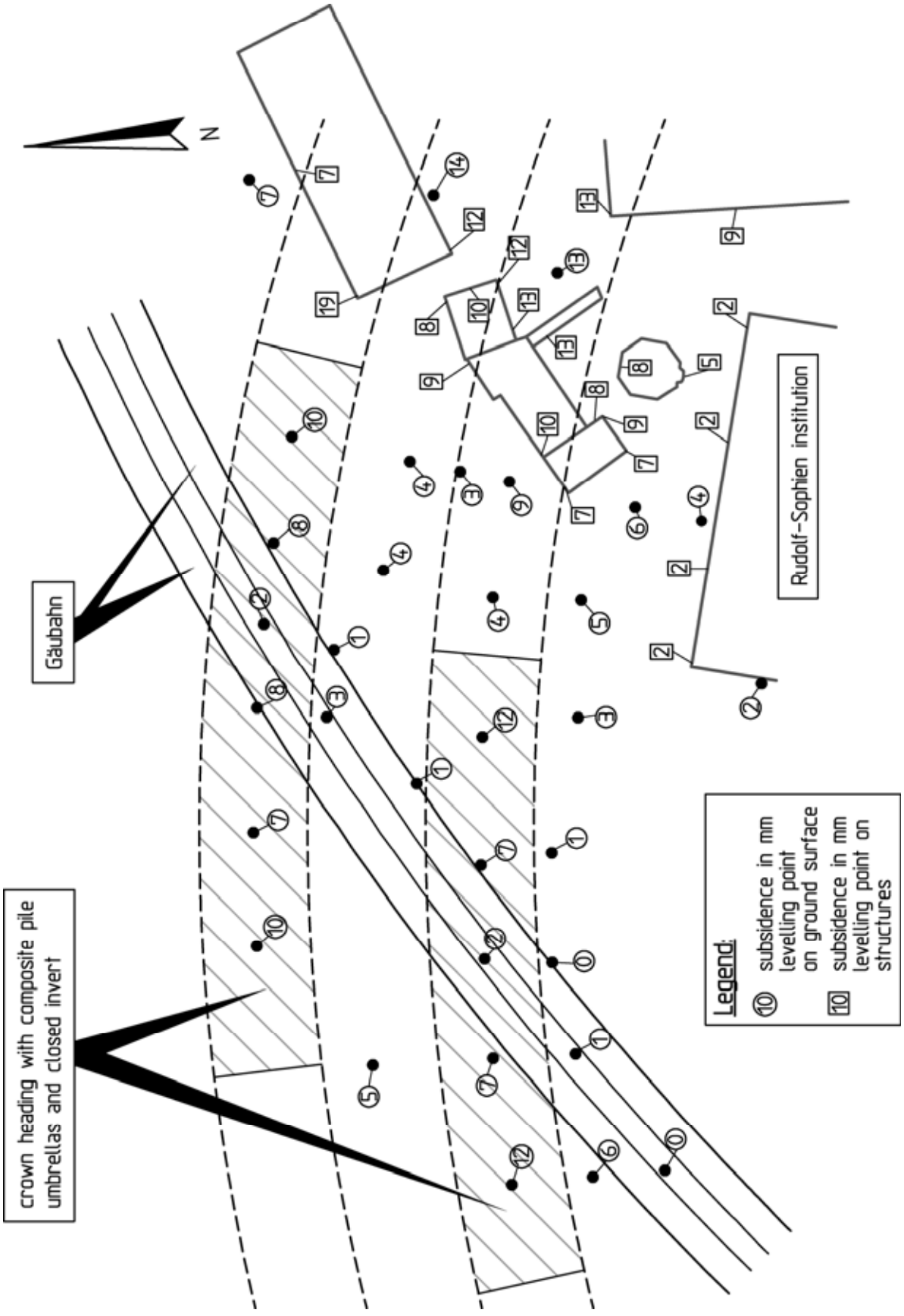

Fig. 3.33: Subsidence of ground surface and structures, measured during crown heading

In both tunnel tubes the crown heading was far ahead of the bench and invert excavation. Fig. 3.33 shows exemplarily the ground surface subsidence due to the crown heading in the area of the undercrossing of the Gäubahn and the buildings adjacent to the Rudolf-Sophien institution. In the area of the undercrossing of the buildings adjacent to the Rudolf-Sophien institution the crown heading was carried out with an open invert and small round lengths of 0.8 to 1.2 m following excavation class 4A-1 (see Fig. 3.26). The subsidence measured here ranges from 7 to 19 mm. In the area of the undercrossing of the Gäubahn the heading was changed over to a crown heading with closed invert under the protection of an advancing support using composite piles and spiles (see Fig. 3.27). The subsidence could thus be limited to 2 to 8 mm. This small subsidence did at no point affect the railway traffic.

The measured ground surface subsidences are in good agreement with the ones determined in the stability analyses. In the area of the undercrossing of the buildings adjacent to the Rudolf-Sophien institution (analysis cross-section AC 2) a maximum surface subsidence of 11 mm was computed (see Fig. 3.31). The maximum surface subsidence computed for the undercrossing of the Gäubahn (analysis cross-section AC 3, see Fig. 3.23) amounts to 7 mm.

3.2.7 Conclusions

With a crown heading with open invert and small round lengths (excavation class 4A-1, see Fig. 3.26) it was possible to achieve small surface subsidence < 2 cm during tunneling in the alternating sequence of sandstone and siltstone horizons of the Stubensandstone formation in the region of Stuttgart.

In order to avoid affecting the railway traffic during the undercrossing of the Gäubahn it was necessary in this area to limit the subsidence to even smaller values. This was achieved mainly by supporting the curved temporary crown invert with shotcrete. For safety reasons an additional advancing support with composite piles was carried out. With a very small surface subsidence ranging from 2 to 8 mm it was possible to maintain the railway traffic without any interference.

In areas where the rock mass could not be excavated by a tunnel excavator smooth blasting was carried out. It was possible to prove by measurements that the vibration velocities fell well be-

low the reference values for the allowable structural vibrations given in DIN 4150, Part 3 (DIN 4150-3, 1999).

The results of the geotechnical monitoring during construction are in good agreement with the surface subsidence computed in the stability analyses. It could thus be shown that FE-analyses are a good basis for estimating the subsidence due to tunneling, if the parameters are assessed appropriate and the excavation and the installation of the support are simulated realistically.

3.3 Hellenberg Tunnel, Germany

3.3.1 Introduction

The alignment of the new railway line Cologne-Rhine/Main runs through the Rhine schist mountains (Rheinisches Schiefergebirge) in NW-SE direction tightly bundled with the freeway (Autobahn) A3. Coming from Cologne, it crosses in particular the Siebengebirge, Westerwald and Taunus mountains. The alignment comprises more than 30 tunnels with a total length of approx. 47 km. The Hellenberg Tunnel is one of six tunnels driven in the Taunus mountains and lies to the south of Idstein.

3.3.2 Structure

The new railway line Cologne-Rhine/Main of German Rail (Deutsche Bahn AG) undercrosses the Hellenberg mountain in a 552 m long tunnel. The maximum overburden of the tunnel amounts to approx. 19 m.

The tunnel sections in the portal areas were constructed by the cut-and-cover method. The central tunnel segment with a length of approx. 470 m was driven by underground construction ascending from southeast to northwest (Fig. 3.34).

A mouth-shaped profile with an excavated width of 15.4 m and a height of 12.3 m was constructed for the double-tracked Hellenberg Tunnel (Fig. 3.35). This is the standard profile for double-Tracked tunnels of the new railway line Cologne-Rhine/Main. The excavated cross-section amounts to approx. 150 m^2 (Fig. 3.35).

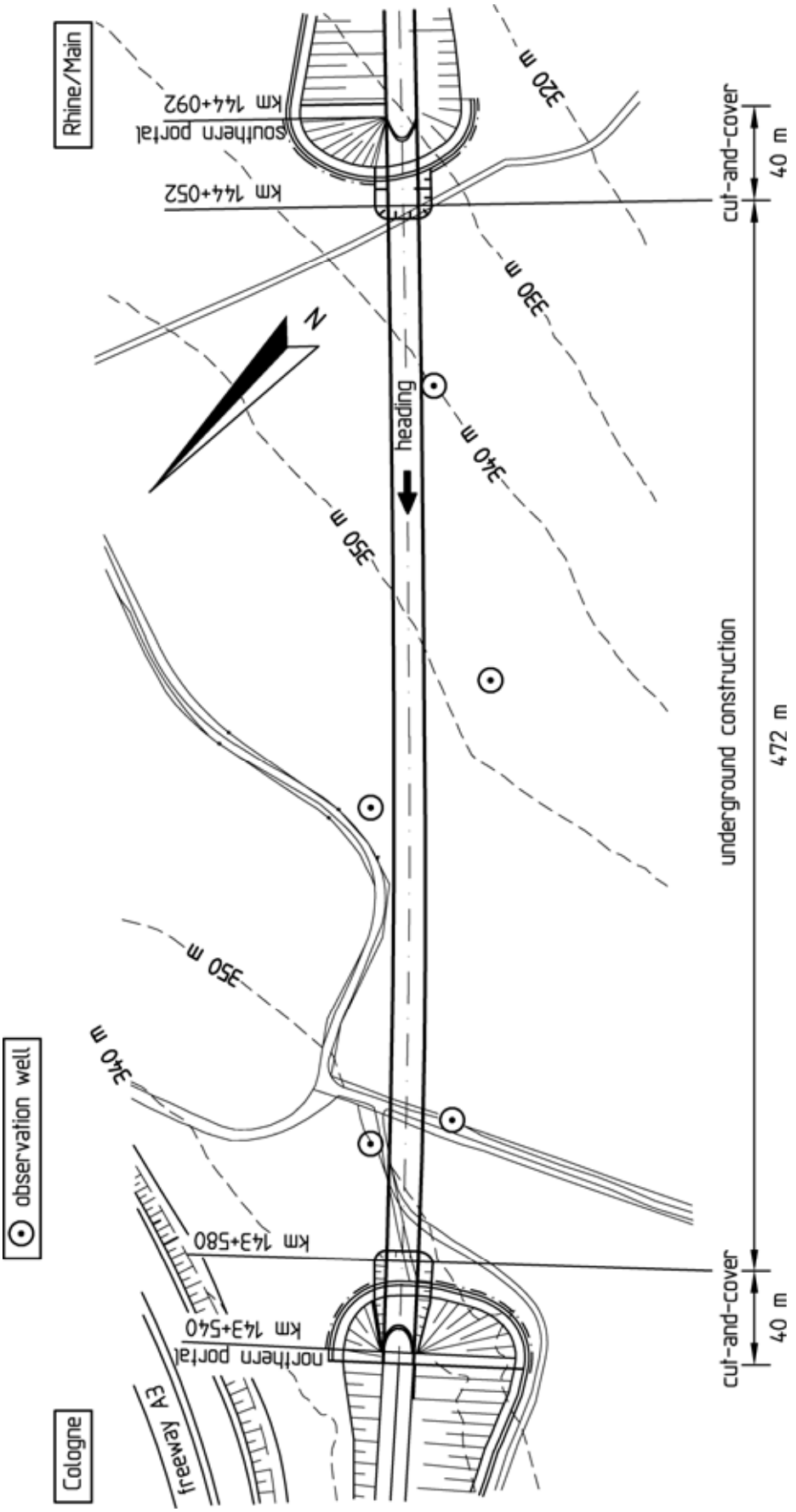

Fig. 3.34: Hellenberg Tunnel, site plan

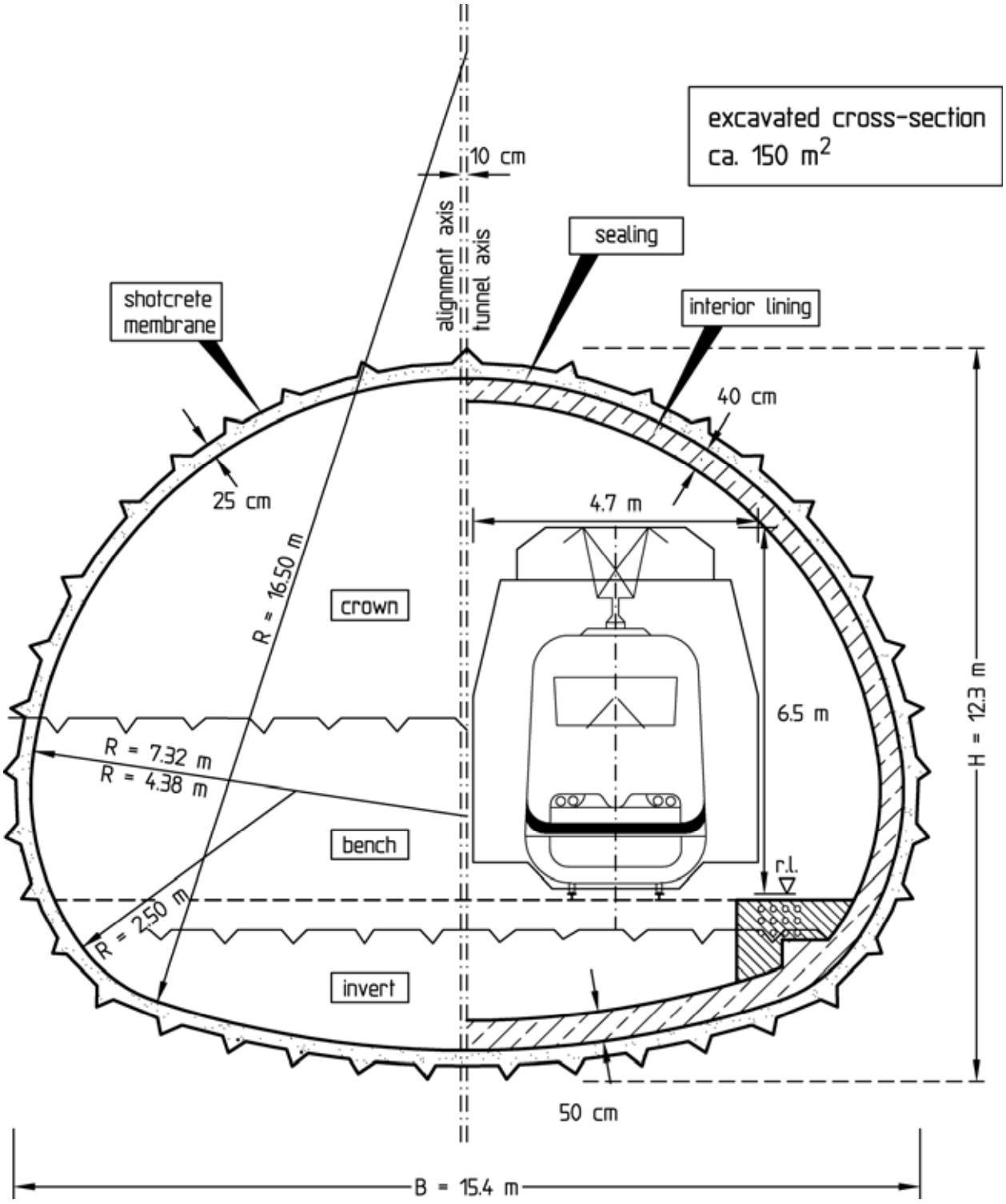

Fig. 3.35: New railway line Cologne-Rhine/Main, standard profile

In the vault area the radius of curvature of the shotcrete membrane amounts to R = 7.32 m. The invert is rounded with a radius of R = 16.5 m. For the transition area from the sidewalls to the

invert radii of R = 4.38 m and R = 2.5 m, respectively, were selected (Fig. 3.35).

Fig. 3.36 shows the southern portal at the start of underground excavation of the Hellenberg Tunnel.

Fig. 3.36: Hellenberg Tunnel, southern portal

3.3.3 Ground and groundwater conditions

The ground along the alignment of the Hellenberg Tunnel was explored by test pits and core drillings. The boreholes were equipped as observation wells (Fig. 3.34 and 3.37).

The Quaternary talus material, which is loamified in the upper region, extends to a depth of approx. 2 m. In the portal areas it is encountered down to a maximum depth of 5 m.

Below the Quaternary cover Devonian rocks follow composed in the area of the Hellenberg Tunnel of phyllitic slate with sandstone and quartzite intercalations and embedded conglomerate lenses. These layers are referred to as Variegated Schist.

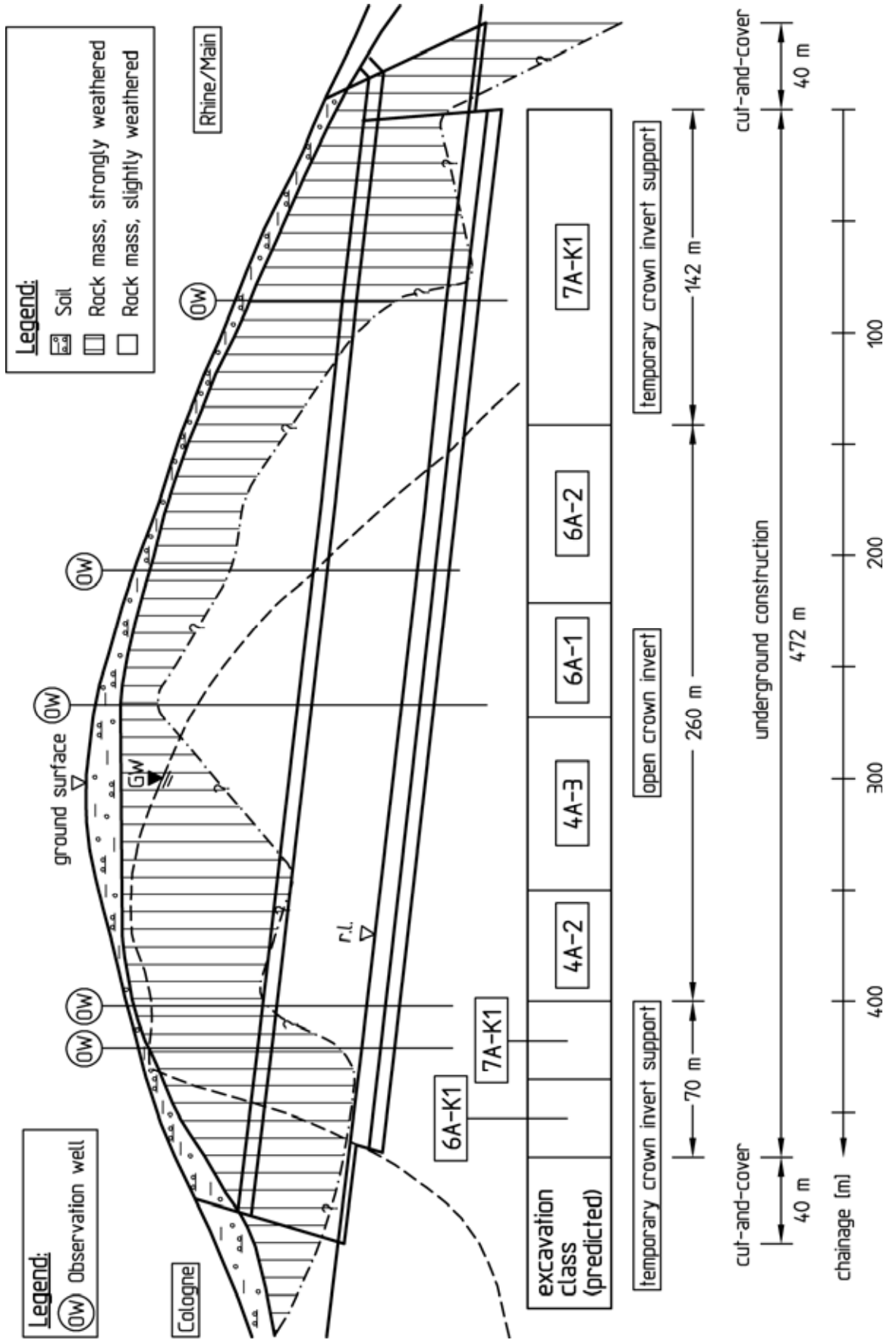

Fig. 3.37: Hellenberg Tunnel, longitudinal section with predicted excavation classes

The rock mass in the area of the Hellenberg Tunnel is characterized by a deep-reaching weathering extending to a depth of some 35 m. Unweathered rock mass is thus only encountered below the tunnel's invert.

In the course of the exploration the drill cores and the test pits were geotechnically mapped. Further, television probing and laboratory and in-situ tests were carried out.

From the northern tunnel portal the groundwater table rises to 12 m above the tunnel roof. In the following, it drops towards the southern tunnel portal to below the tunnel's invert. The groundwater table mapped in the tunnel's longitudinal section (Fig. 3.37) is based on the highest groundwater levels measured in the boreholes equipped as observation wells.

3.3.4 Excavation classes

Because of the size of the excavation profile it was necessary to subdivide excavation and support into crown, bench and invert (Fig. 3.35). An advancing crown excavation was carried out.

A prediction of the distribution of the excavation classes based on the results of the exploration and of stability analyses and on experience is shown in Fig. 3.37. According to the drilling results, the strongly weathered rock extends in the portal areas to about the tunnel's invert. Accordingly, excavation classed with a temporary crown invert support were planned here (6A-K1 and 7A-K1, see DGGT, 1995: Table 1). In the central tunnel section it was expected that the crown heading can be carried out with an open invert. In parts excavation classes without advance support measures (4A-2 and 4A-3, see DGGT, 1995: Table 1) were predicted. For other sections it was assumed that the heading requires advance support (excavation classes 6A-1 and 6A-2, see DGGT, 1995: Table 1).

The excavation methods, round lengths and support measures planned for excavation classes 6A-1 and 6A-2 are shown in Fig. 3.38 and 3.39.

It was planned to carry out the excavation mainly by tunnel excavators and hydraulic chisels. In areas in which the tunnel was located in slightly weathered and slightly jointed rock, local loosening blasting was planned.

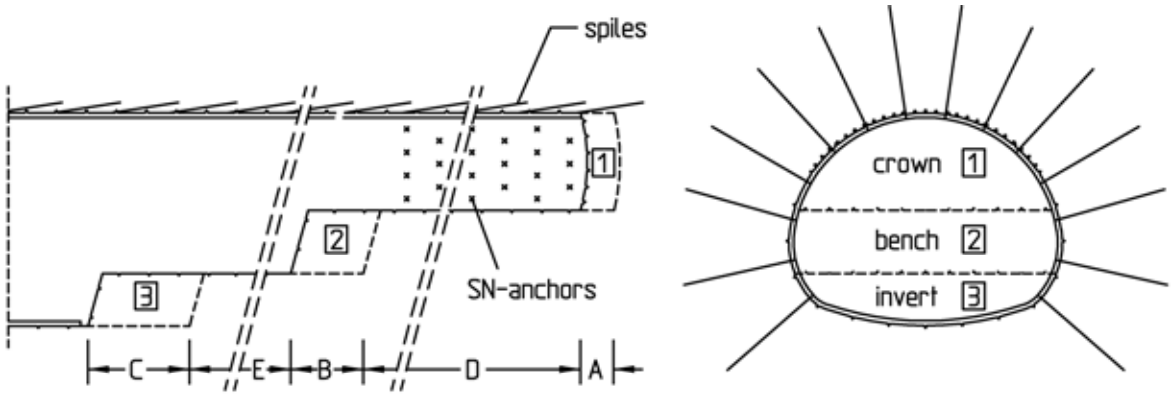

Excavation class		6A-1	6A-2
Excavation method		tunnel excavator + hydraulic chisel local loosening blasting	tunnel excavator + hydraulic chisel local loosening blasting
Unsupported round length	crown (A) bench (B) invert (C)	0.80 - 1.20 m 1.60 - 2.40 m ≦ 3.60 m	1.21 - 1.60 m 2.41 - 3.20 m ≦ 4.80 m
Tunnel face support		none	none
Advance support		mortar spiles $l_S \geqq 3$ m, $d_S \leqq 30$ cm	mortar spiles $l_S \geqq 4$ m, $d_S \leqq 30$ cm
Shotcrete B25	vault crown invert	25 cm -	25 cm -
Reinforcement	vault	steel fabric mats (2 layers)	steel fabric mats (2 layers)
Systematic anchoring		l_A = 4 m, min. 12 pcs./round	l_A = 4 m, min. 12 pcs./round
Steel set spacing	crown bench	0.80 - 1.20 m 1.60 - 2.40 m	1.21 - 1.60 m 2.41 - 3.20 m
Trailing distance	bench (D) invert (E)	depending on the monitoring results, the encountered geotechnical conditions and supplementary FE-analyses	

Fig. 3.38: Excavation classes 6A-1 and 6A-2

The unsupported round lengths during the crown excavation were specified in excavation class 6A-1 as 0.80 to 1.20 m and in excavation class 6A-2 as 1.21 to 1.60 m (Fig. 3.38 and 3.39). In both excavation classes an advance support of the crown with 3 to 4 m long mortar spiles was provided for (Fig. 3.38 and 3.39). Shotcrete of grade B25 was selected for the shotcrete membrane at a thickness of 25 cm and reinforced inside and outside by steel fabric mats Q221 (Fig. 3.38 and 3.39). In the sidewall area a systematic anchoring with at least twelve 4 m long SN-anchors per tunnel meter was planned (Fig. 3.38 and 3.39).

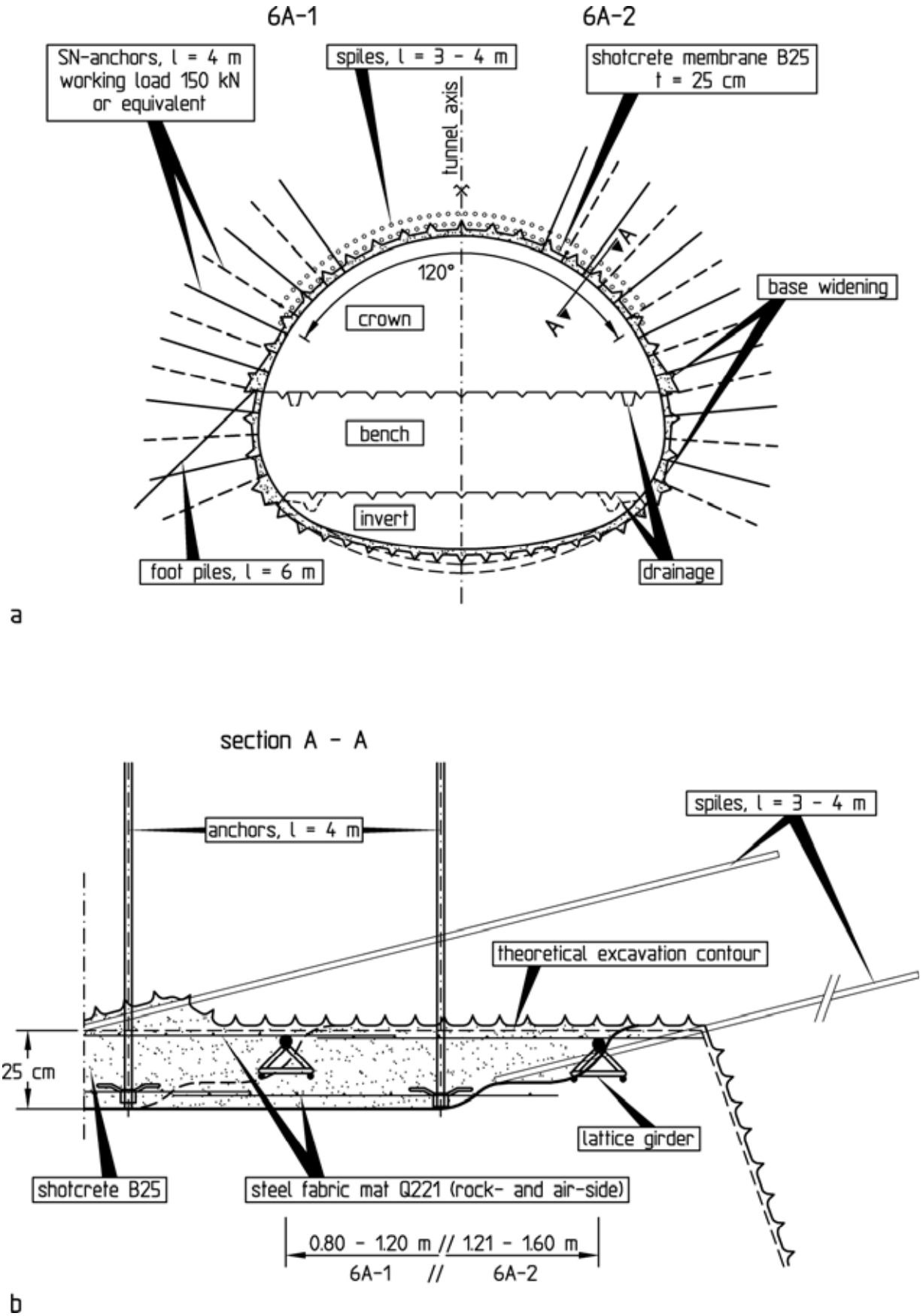

Fig. 3.39: Support for excavation classes 6A-1 and 6A-2: a) Cross-section; b) longitudinal section

A possible installation of anchors in the roof area ought to be decided on site. For each round one steel set (lattice girder) was to be installed in the crown area (Fig. 3.38 and 3.39).

The trailing distance of the bench (section D in Fig. 3.38) and the closing of the invert (section E in Fig. 3.38) was to be specified depending on the results of monitoring during heading, the encountered geotechnical conditions and the results of the stability analyses.

The unsupported round lengths were specified in excavation class 6A-1 for the bench and the invert as 1.60 to 2.40 m and ≤ 3.60 m, respectively. In excavation class 6A-2 the corresponding round lengths amounted to 2.41 to 3.20 m and ≤ 4.80 m, respectively (Fig. 3.38).

To improve the stability, the shotcrete membrane was to be widened to t = 60 cm in the area of the crown and bench support feet if necessary. It is shown calculational in Wittke et al. (1986), Wittke (1990) and Wittke (1998), however, that the stability of a crown heading with open invert can only slightly be improved by these kind of measures.

3.3.5 Crown heading

The excavation classes were finally specified during the crown heading on the basis of the results of stability analyses, of crown face mappings (see Chapter 3.3.6) and of the monitoring results.

The crown was excavated over the entire tunnel length without a trailing bench excavation (unlimited length of section D in Fig. 3.38). In the area of the southern portal a crown heading with a temporary support of the invert was carried out over a length of approx. 80 m (excavation class 7A-K1, Fig. 3.40). At the northern portal a temporary support of the invert was only constructed in the beginning of excavation (excavation class 6A-K1, Fig. 3.40).

In the remaining area a crown heading with open invert was carried out (excavation classes 6A-1 and 6A-2, Fig. 3.40).

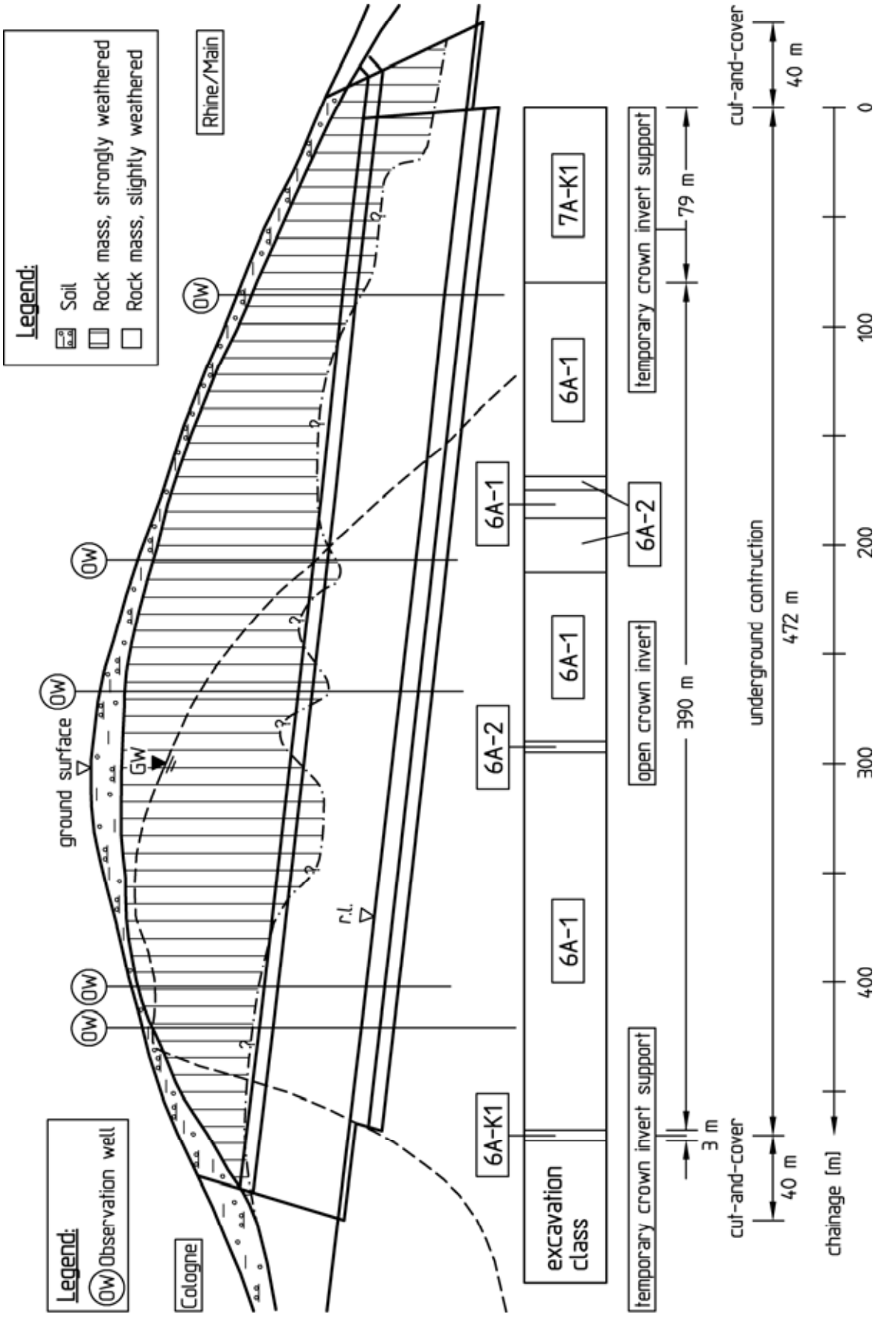

Fig. 3.40: Hellenberg Tunnel, longitudinal section and excavation classes, as carried out

3.3.6 Results of the crown face mapping

The evaluation of the crown face mapping resulted in a modified elevation of the boundary between strongly and slightly weathered rock as compared to the exploration results (Fig. 3.37 and 3.40). Nevertheless, the predicted distribution of excavation classes agreed well with the construction (Fig. 3.37 and 3.40).

During the tunnel face mapping the appearance, the extent and the orientation of the discontinuities were determined as well.

Fig. 3.41 shows as an example the crown face mapping at chainage 345.4 m. The strike and dip angles of the discontinuities were measured using a geological compass (see Chapter 2.5.1). For reasons of clarity of the representation only some of the measured discontinuity orientations are mapped in Fig. 3.41.

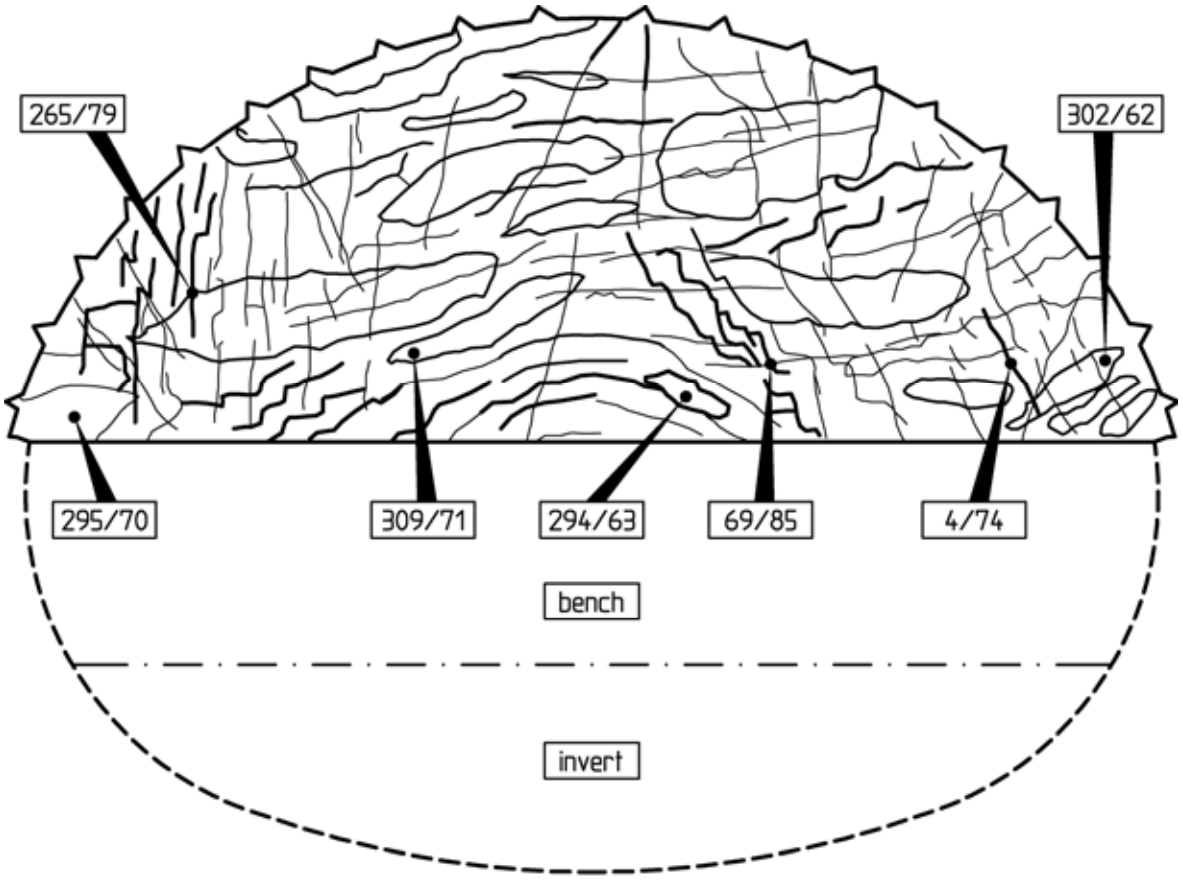

Fig. 3.41: Crown face mapping, chainage 345.4 m

In Fig. 3.42 all discontinuity orientations measured from chainage 300 to 350 m are shown in a polar diagram (see Chapter 2.5.1). Accordingly the discontinuities can mainly be assigned to three sets.

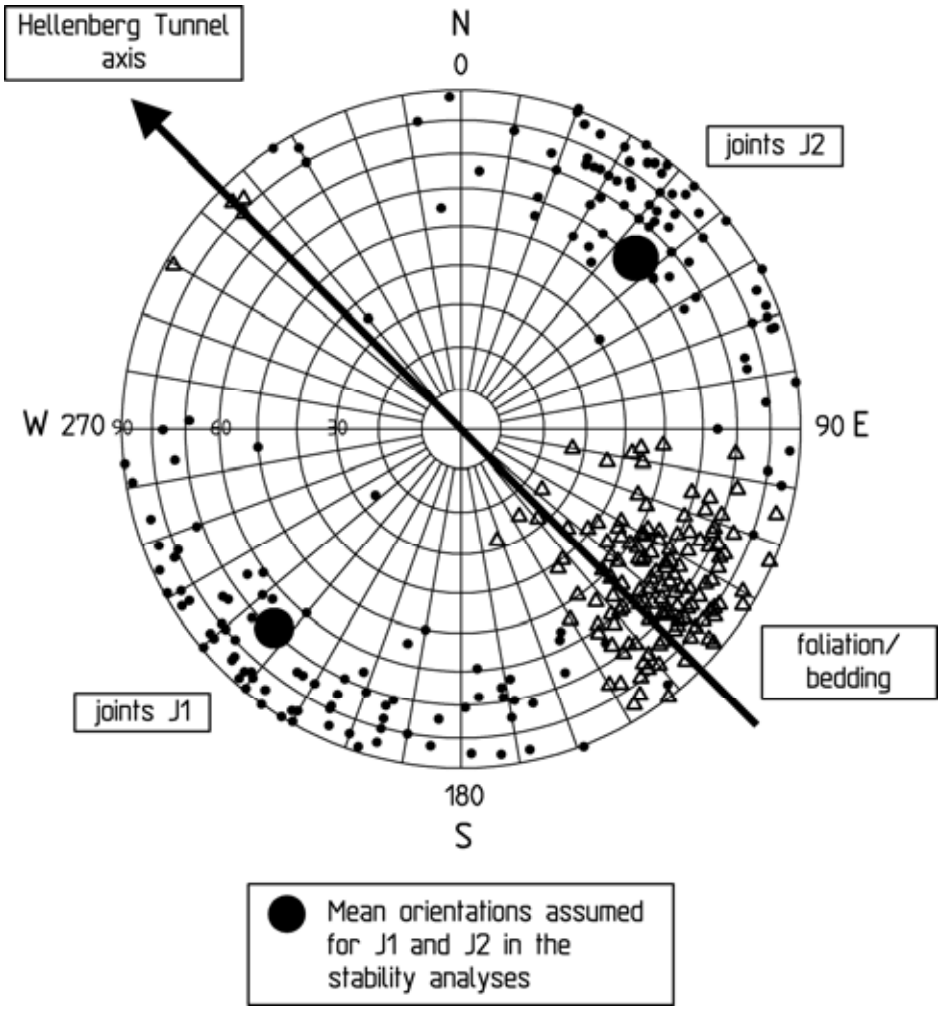

Fig. 3.42: Measured discontinuity orientations, chainage 300 to 350 m, polar diagram

The bedding planes and foliation discontinuities display the NE-SW strike typical for the Rhine schist mountains and dip at a moderate steep to steep angle (50 to 80°) towards northwestern directions. Two joint sets J1 and J2 further exist dipping mostly steeply (60 to 90°) and striking parallel to the tunnel axis (Fig. 3.42).

Fig. 3.43 shows the bench at the southern portal. The photograph gives an impression of the strongly weathered rock in this area and of the discontinuity fabric.

Fig. 3.43: Bench at the southern portal

3.3.7 Stability analyses for the bench excavation

Within the tunnel sections driven according to excavation classes 6A-1 and 6A-2 an advancing crown excavation with open invert and trailing bench and invert excavation was planned (Fig. 3.38). The evaluation of the mapping carried out during the crown heading revealed, however, that the steep joints J1 and J2 striking parallel to acute-angled to the tunnel axis (see Fig. 3.42) appear frequently in some areas and have a large extent. Before the start of the bench excavation the stability of the tunnel in this construction stage was therefore investigated in FE-analyses with the program system FEST03 (Wittke, 2000). On the basis of the results of these analyses the length of the section E between bench and invert excavation (see Fig. 3.38) was to be specified.

Fig. 3.44 shows the computation section, the FE-mesh, the ground profile and the parameters taken as a basis for the stability analyses (Wittke et al., 1999). The tunnel cross-section is located in the strongly to slightly weathered Variegated Schist. The overburden is 18 m high. Below the tunnel's invert the rock is unweathered.

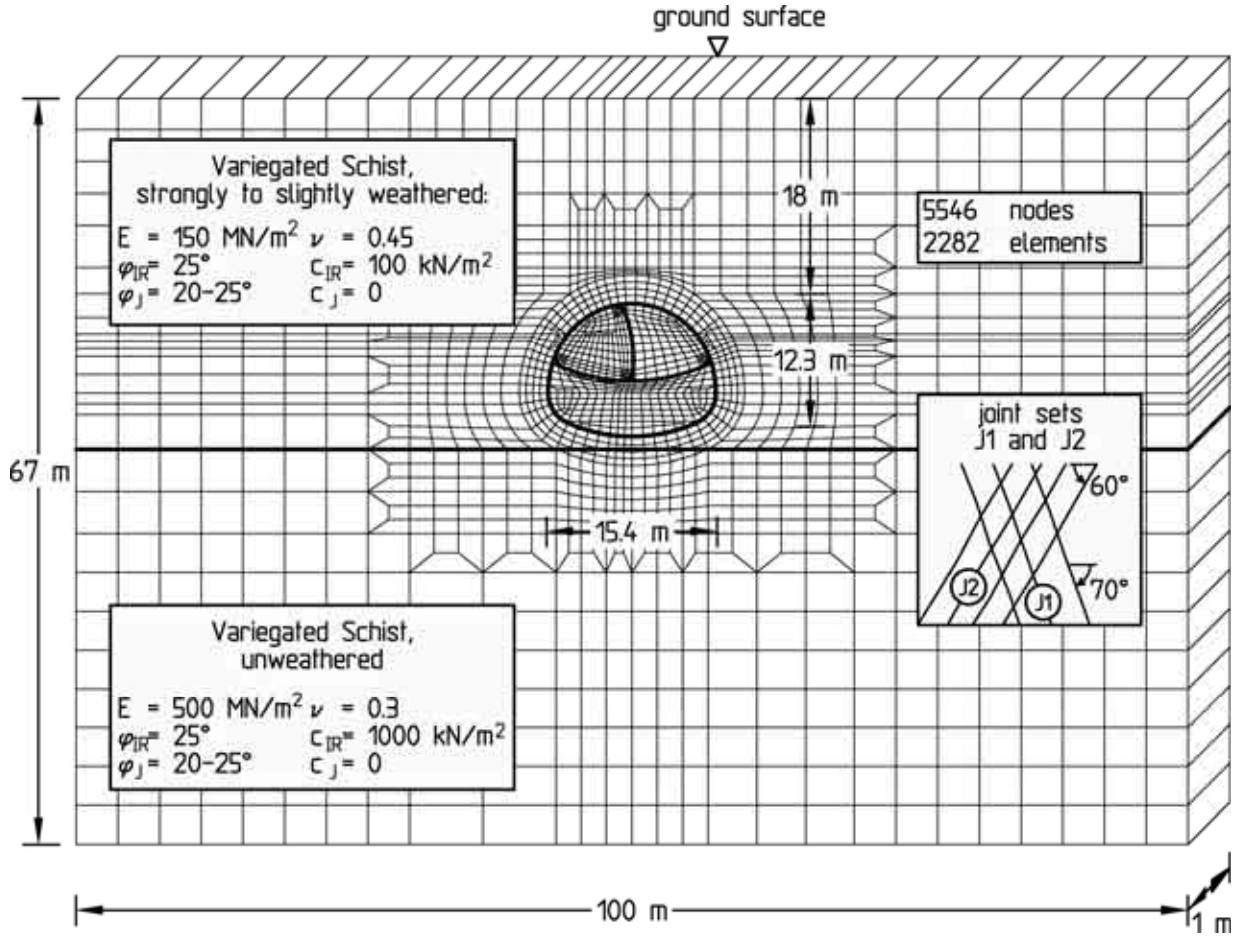

Fig. 3.44: Computation section, FE-mesh, ground profile and parameters

As mentioned above, the foliation or bedding, respectively, strikes approx. perpendicularly to the tunnel axis and dips steeply (see Fig. 3.42). Since discontinuities of this orientation hardly influence the load transfer in transverse tunnel direction, the foliation/bedding was not taken into account in the analyses. The shear strength of the joints J1 and J2, which are relevant for the stability, was, however, accounted for. The shear strength was furthermore varied because of the different appearance of these discontinuities. Three cases were investigated, in which the friction angles on the joints φ_J were assumed as 20°, 22.5° and 25° and the cohesion as $c_J = 0$. The anchoring of the rock provided for in all excavation classes was not taken into account in the analyses as a conservative assumption.

The heading of the tunnel was simulated in four computation steps (Fig. 3.45). In the 1st computation step the in-situ state of stress and deformation resulting from the dead weight of the rock mass was computed. After that, the excavation of the crown (2nd

computation step) and the bench (3rd computation step) was simulated, each time with simultaneous installation of the shotcrete membrane. In the 4th computation step the invert was excavated and supported using shotcrete.

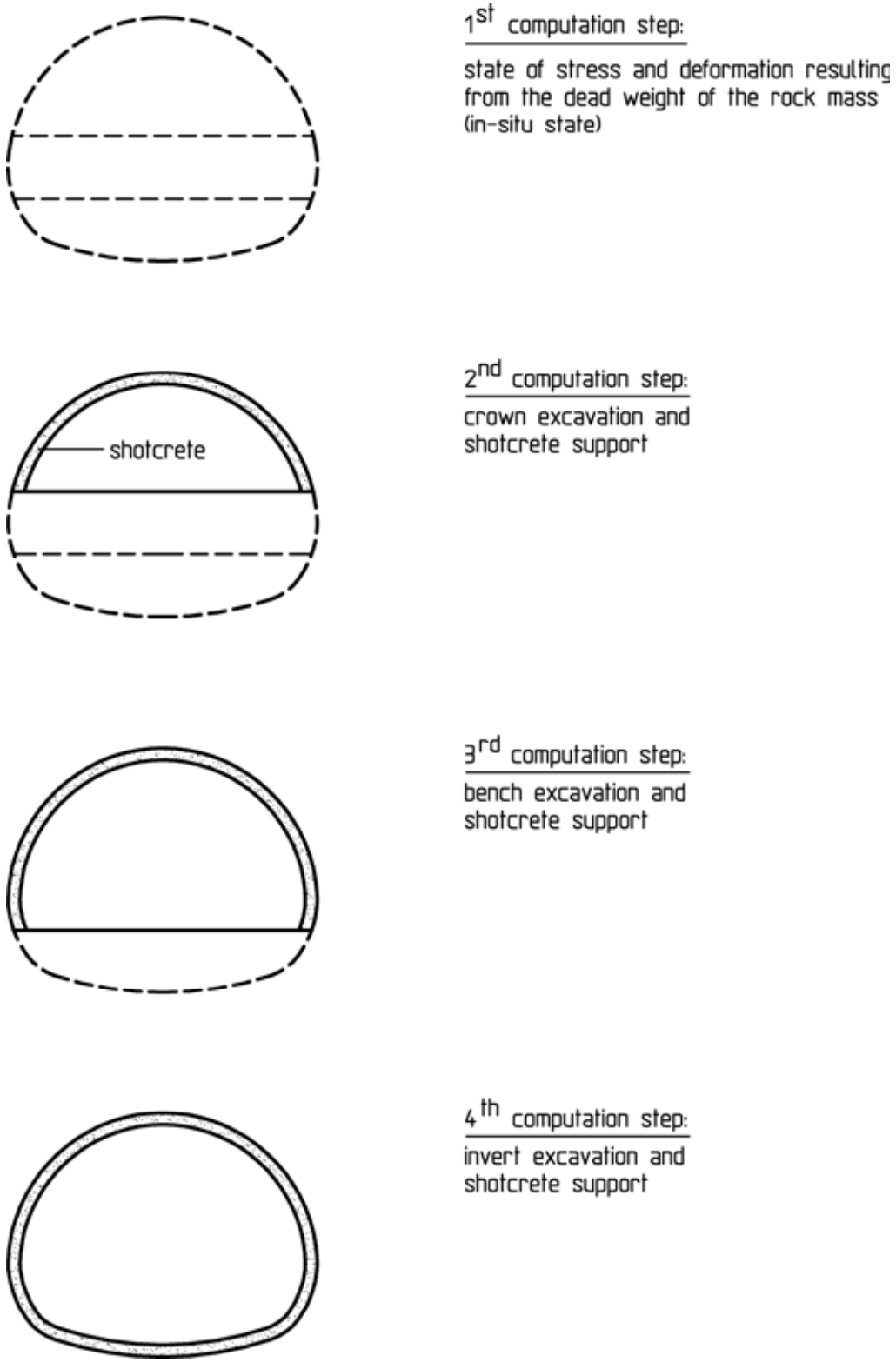

Fig. 3.45: Computation steps

A thickness of t = 25 cm (see Fig. 3.35) and a Young's modulus of E = 15,000 MN/m^2 were specified for the shotcrete membrane.

Fig. 3.46 shows the development of the displacements computed for the bench support feet in the course of the viscoplastic iterative analysis in the 3rd computation step.

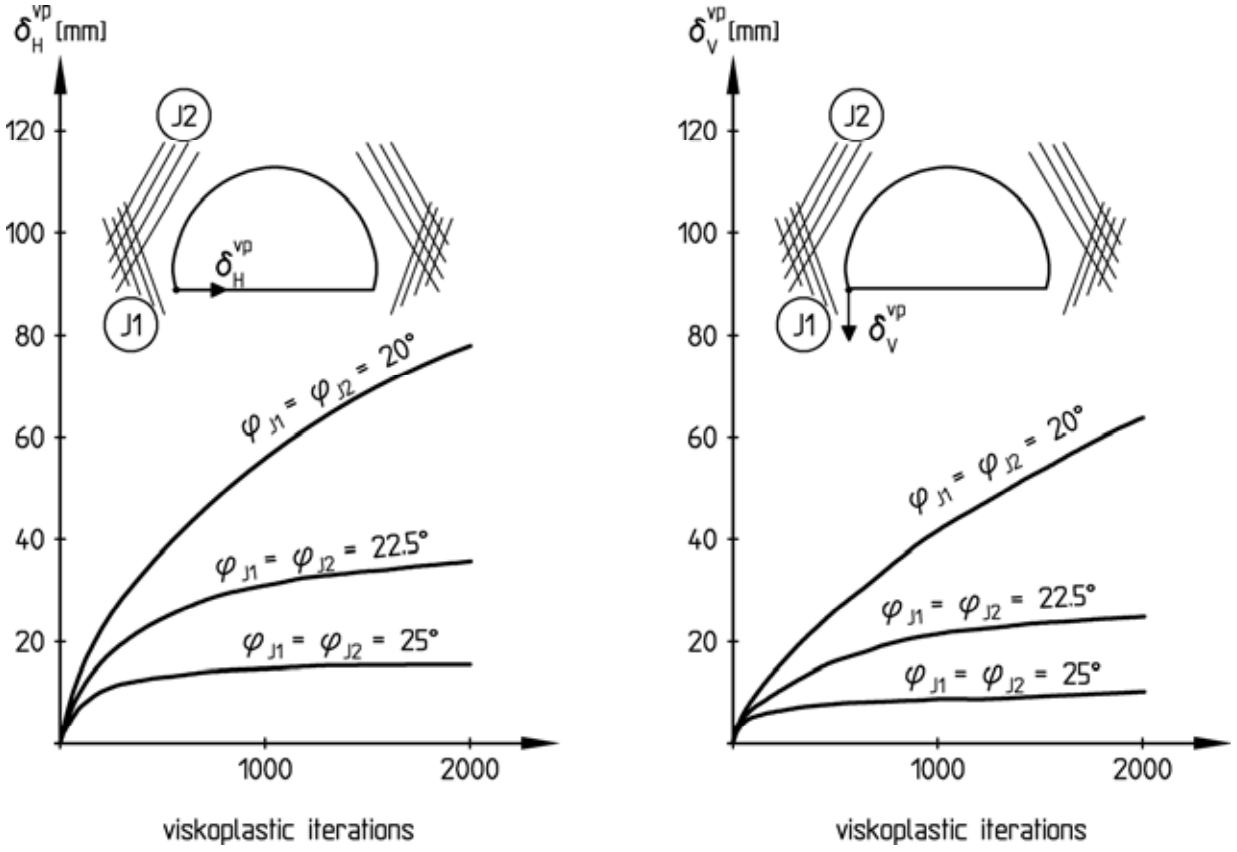

Fig. 3.46: Viscoplastic displacements depending on the shear strength of the joint sets J1 and J2, 3rd computation step

For the case φ_J = 25° the stability of the construction stage due to the bench excavation can be proven in the analysis. The horizontal and vertical displacements computed at the bench support feet converge in the course of the viscoplastic iterative analysis (see Fig. 3.46). The horizontal and vertical components of the viscoplastic displacements of the bench support feet amount to δ_H^{vp} = 15.6 mm and δ_V^{vp} = 9.2 mm.

With decreasing friction angle φ_J markedly larger viscoplastic displacements are computed (see Fig. 3.46). In the case φ_J = 20° the displacements do not converge in the analysis (see Fig. 3.46). The

stability of the construction stage as a result of the bench excavation can thus not be proven by the analysis for this case.

Summarizing it may be stated that the stability of the tunnel during bench excavation depends to a large degree on the friction angle φ_J on the joints.

On the basis of the results of the stability analyses it was agreed upon for those sections in which the crown was excavated without invert support to set no limit for the length of the section E between bench excavation and the support of the invert (see Fig. 3.38). With the bench mapping during heading, however, great importance was attached to recording the appearance and extent of the joints. Whenever strongly jointed rock was encountered during bench excavation, the anchoring of the sidewalls was intensified.

3.3.8 Construction and monitoring results

Fig. 3.47 shows the sequence of the heading. Following the crown heading (1), the bench was excavated up to chainage approx. 80 m at a round length of 2.0 m. The invert trailed with a round length of 3.6 m and was supported after each round (2). In this area the strongly weathered rock mass extends into the tunnel cross-section (Fig. 3.47), and a crown invert support was installed.

After that, the bench was excavated from chainage 80 m to 462 m with a round length of 2.4 m (3 in Fig. 3.47). As mentioned, the anchoring was locally intensified because of the heavy jointing of the rock mass.

In the northern portal area the bench was excavated again with immediately trailing invert over a short tunnel section (4 in Fig. 3.47). The round lengths were the same as in the southern portal area.

Finally, the invert was excavated backward and supported with round lengths of 3.6 m (5 in Fig. 3.47).

The heading was accompanied by a geotechnical monitoring program including surface leveling, extensometer and inclinometer measurements from the ground surface and leveling and convergency measurements in the tunnel.

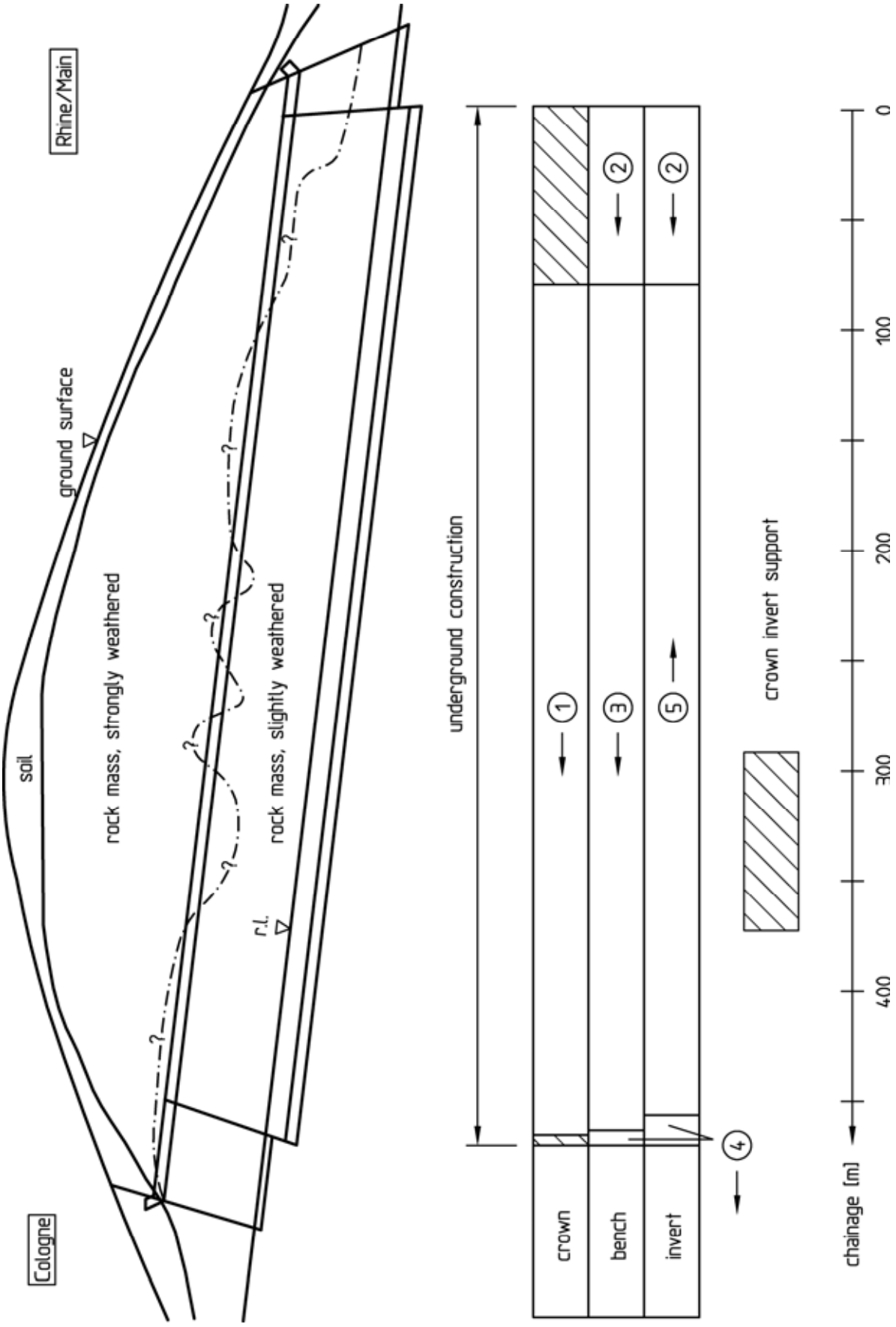

Fig. 3.47: Excavation, heading sequence

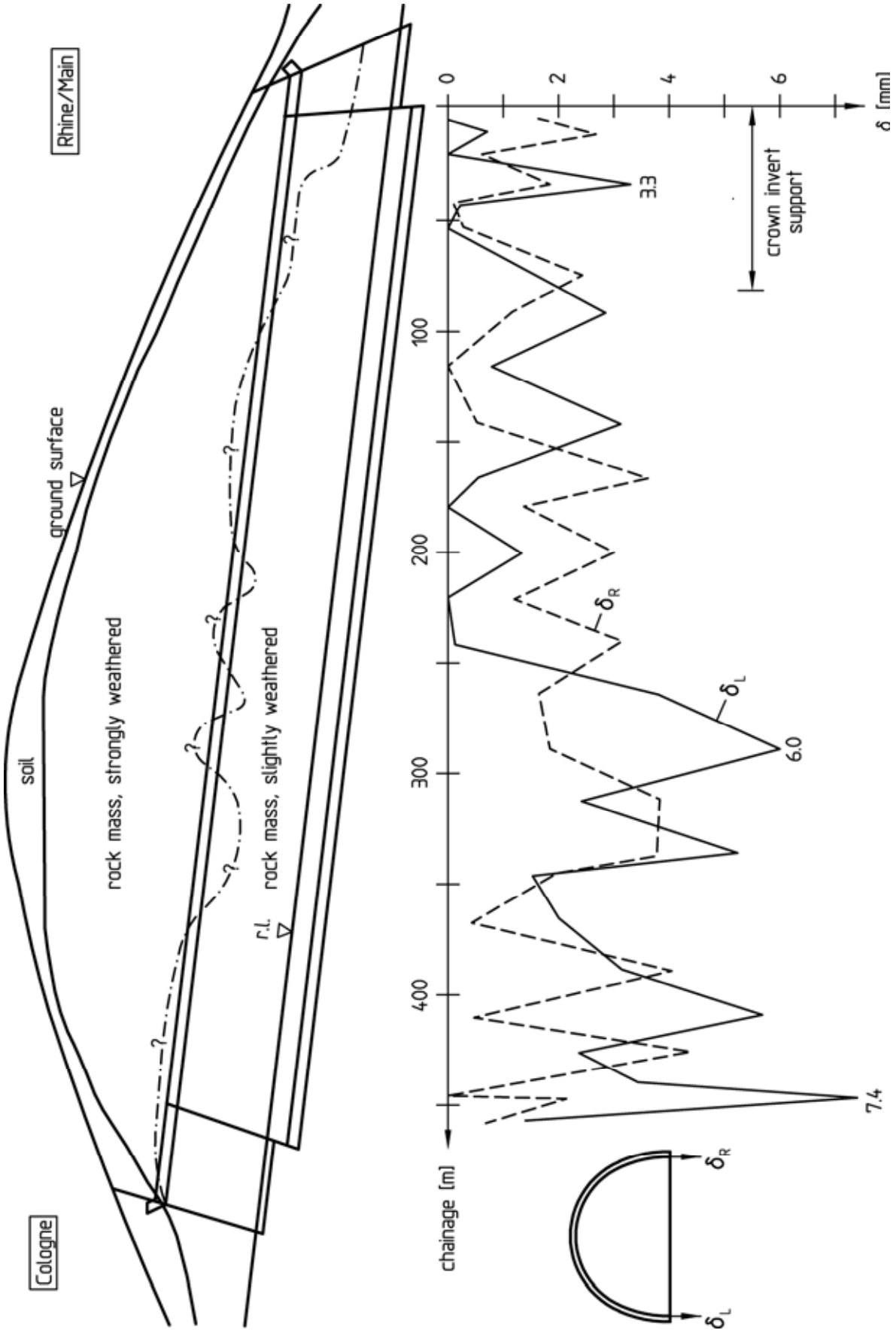

Fig. 3.48: Measured vertical displacements at the bench support feet

Fig. 3.48 shows exemplarily the maximum subsidence at the bench support feet measured after bench excavation. Since the elastic part of the displacements had mostly occurred already before the zero reading, it could not be recorded by the measurements. The measurement results were therefore compared to the computed viscoplastic displacement parts shown in Fig. 3.46. It becomes apparent that the measured displacements are smaller than the viscoplastic vertical displacements computed assuming a friction angle of $\varphi_J = 25^\circ$ (approx. 10 mm). It thus turns out that the construction stage following the bench excavation was stable as predicted.

3.3.9 Conclusions

Crown headings are carried out in excavation classes with and without invert support, depending on the rock conditions. Since the different excavation classes vary strongly in cost, great importance is attached to the appropriate specification. The example of the Hellenberg Tunnel shows how the excavation classes can be specified safely on the basis of the results of stability analyses, mapping during construction and monitoring. It becomes apparent that proofs of stability according to the FE-method can contribute essentially towards the prediction of and decision on the excavation classes.